

ABUNDANCE AND SPECIATION OF GOLD IN MASSIVE SULFIDES OF THE BATHURST MINING CAMP, NEW BRUNSWICK, CANADA

SEAN H. McCLENAGHAN[§] AND DAVID R. LENTZ

Department of Geology, University of New Brunswick, Fredericton, New Brunswick E3B 5A3, Canada

LOUIS J. CABRI

*99 Fifth Avenue, Suite 122, Ottawa, Ontario K1S 5P5, and Department of Earth Sciences,
Memorial University of Newfoundland, St. John's, Newfoundland A1B 3X5, Canada*

ABSTRACT

Massive sulfide deposits of Zn–Pb–Cu–Ag type in the Bathurst Mining Camp, New Brunswick, are hosted within a Middle Ordovician bimodal volcanic and sedimentary sequence that has undergone complex polyphase deformation and associated regional metamorphism to the lower- to upper-greenschist grade. These factors are partly responsible for the present geometry and textural modification of these hydrothermal deposits, originally formed on the seafloor. Despite the importance of heterogeneous ductile deformation, some primary features are evident, in particular fine-grained colloform pyrite and base- and precious-metal zonation within many of these deposits. The average Au content (bulk instrumental neutron-activation analyses; $n = 215$) of massive sulfides from 43 deposits in the Bathurst Mining Camp is 0.85 ppm, with values as high as 6.86 ppm. Positive correlations of Au content with Ag ($r' = 0.53$), As ($r' = 0.57$) and Sb ($r' = 0.65$) suggest that Au is mainly associated with arsenian pyrite and a distal suite of elements (Au + Sb + As \pm Ag). The submicroscopic Au contents of pyrite and arsenopyrite in eight deposits with elevated bulk Au contents were investigated using a Cameca IMS-4f secondary-ion mass spectrometer. Results suggest that arsenian pyrite is the most important host for Au in massive sulfides of the Bathurst Mining Camp, with an average Au content of 9.1 ppm, and values reaching 42.9 ppm. Arsenopyrite was found to contain much less Au, with an average of 2.7 ppm. Recrystallization of sulfides during greenschist-facies metamorphism has resulted in pyrite morphologies with variable Au contents. Invisible Au was in part released and adsorbed as submicroscopic inclusions on As-rich surfaces of pyrite and on arsenopyrite.

Keywords: gold, massive sulfides, electron-microprobe data, ion-microprobe data, Bathurst Mining Camp, New Brunswick.

SOMMAIRE

Les gisements de sulfures massifs de Zn, Pb, Cu et Ag du camp minier de Bathurst, au Nouveau-Brunswick, sont situés dans un ensemble ordovicien moyen de roches volcaniques et sédimentaires bimodales qui ont subi les effets d'une déformation polyphasée complexe et d'une recristallisation métamorphique régionale associée, jusqu'au faciès schistes verts supérieur. Ces facteurs sont en partie responsables de la géométrie actuelle et des modifications texturales de ces gisements hydrothermaux, formés sur le fond de la mer. Malgré l'importance d'une déformation ductile hétérogène, certaines caractéristiques primaires sont évidentes, en particulier la pyrite colloforme à granulométrie fine et la zonation en métaux de base et métaux précieux dans plusieurs de ces gisements. La teneur moyenne en or, déterminée par activation neutronique instrumentale ($n = 215$) de sulfures massifs provenant de 43 gîtes, est 0.85 ppm, avec des valeurs atteignant 6.86 ppm. Des corrélations positives de la teneur en or avec celles de Ag ($r' = 0.53$), As ($r' = 0.57$) et Sb ($r' = 0.65$) font penser que l'or est surtout associé à la pyrite arsénienne et à une suite d'éléments (Au + Sb + As \pm Ag) enrichis dans les parties distales des systèmes minéralisés. Les teneurs en or submicroscopique de la pyrite et l'arsénopyrite dans huit gisements à teneurs élevées en or ont été déterminées au moyen d'une microsonde ionique Cameca IMS-4f avec spectrométrie de masse. Les résultats montrent que la pyrite arsénienne est l'hôte le plus important de l'or dans les sulfures massifs de ce camp minier, avec en moyenne 9.1 ppm, et des valeurs atteignant 42.9 ppm. L'arsénopyrite contient beaucoup moins d'or, en moyenne 2.7 ppm. La recristallisation des sulfures au cours du métamorphisme a donné des morphologies de pyrite à teneurs variables en Au. De plus, l'or invisible a été libéré en partie et adsorbé sous forme d'inclusions submicroscopiques sur les surfaces de la pyrite enrichies en arsenic et de l'arsénopyrite.

(Traduit par la Rédaction)

Mots-clés: or, sulfures massifs, données de microsonde électronique, données de microsonde ionique, camp minier de Bathurst, Nouveau-Brunswick.

[§] E-mail address: ventcomplex@hotmail.com

INTRODUCTION

The Bathurst Mining Camp (BMC), situated in northeastern New Brunswick (Fig. 1), eastern Canada, contains 24 deposits with individual geological reserves exceeding 1.0 Mt in addition to over 100 smaller deposits and occurrences (Goodfellow & McCutcheon 2003). The BMC has been a significant producer of Zn, Pb, Cu and Ag, with past production coming from Brunswick No. 12, No. 6, Captain North Extension, Wedge, Heath Steele, Stratmat, Caribou and Restigouche deposits. The 230 Mt Brunswick No. 12 deposit has produced over 106 Mt of massive sulfides grading 3.49% Pb, 8.85% Zn, 0.36% Cu, 102 ppm Ag and 0.67 ppm Au. The average Au content of massive sulfides (average result of bulk instrumental neutron-activation analyses; $n = 215$) from 43 massive sulfide deposits in the BMC is 0.85 ppm, with values ranging from a detection limit of 0.002 ppm to 6.86 ppm Au (McClenaghan *et al.* 2003).

Gold in massive sulfides of the BMC has never been exploited directly, although it has been recovered as a by-product during smelting. Historically, Au production has come exclusively from gossans and supergene zones that are known to overlie nine ore bodies in the BMC (Luff 1995). The largest known gossan zone in the BMC overlies the Murray Brook deposit (Boyle 1995). Between 1989 and 1992, a total of 10.7 million grams of Ag and 1.3 million grams of Au were recovered by Nova Gold Resources Ltd. (Burton 1993). Similar gossans overlying the Caribou and Heath Steele deposits were also exploited for Au and Ag between 1982 and 1984 (Cavelero 1993, Luff 1995).

Leblanc (1989) and Chryssoulis & Agha (1990) have described the form of gold in bulk samples of sulfide from the Brunswick No. 12 deposit. However, the mineralogical distribution of gold in other BMC deposits has never been investigated. In this paper, we present results of secondary-ion mass spectrometry (SIMS) analyses of pyrite and arsenopyrite in eight massive sulfide deposits from the BMC. This research forms a component of a larger study documenting the form, distribution and genesis of gold in massive sulfide deposits of the BMC (McClenaghan 2002).

BACKGROUND INFORMATION

Geological setting of massive sulfide deposits

Massive sulfide deposits in the Bathurst Mining Camp are hosted by Ordovician felsic volcanic and sedimentary rocks of the Bathurst Supergroup, with the most voluminous accumulations of sulfides occurring in four key horizons: Brunswick, Heath Steele, Caribou and Stratmat (Fig. 1). The massive sulfide deposits consist of fine-grained, layered stratiform lenses comprising pyrite, sphalerite, galena, chalcopyrite and pyrrhotite with minor arsenopyrite, marcasite and tetrahedrite.

Sulfide layering, best developed in the Pb- and Zn-rich lenses (Fig. 2a), is a result of compositional and grain-size variations in sulfide minerals brought about by synmetamorphic deformation (McAllister 1960, Stanton 1960). Stringer mineralization underlies most deposits (Fig. 2b), with a distinct feeder zone having been recognized at numerous deposits, including Brunswick No. 12 (Luff *et al.* 1992, Lentz & Goodfellow 1993a, b), Halfmile Lake (Adair 1992) and Caribou (Goodfellow 2003). Large alteration-induced halos associated with stockwork mineralization are present in sedimentary and volcanic rocks in the footwall to these deposits, and are interpreted to be the signs of the circulation of hydrothermal fluid in the footwall during the formation of massive sulfide deposits (Goodfellow 1975, Lentz & Goodfellow 1993a, b). Interaction of high-temperature hydrothermal fluids with massive sulfides, at the base of the sulfide lenses, has also metasomatically transformed the sulfides into a high-temperature assemblage composed of pyrite, pyrrhotite and chalcopyrite (Fig. 2c), hereafter referred to as the basal sulfide facies.

The entire sequence was subjected to ductile deformation and associated lower- to upper-greenschist and blueschist metamorphism during closure of the Tetagouche-Exploits back-arc basin in the Ordovician to Late Silurian (van Staal & Fyffe 1991). Intense thrusting imbricated these rocks into thrust blocks now juxtaposed against each other, and subsequently folded them into shallow and steep structures. Massive sulfides in the BMC have been modified by widespread greenschist-facies metamorphism increasing from lower- to upper-greenschist grade from northeast to southwest (Helmstaedt 1973, van Staal 1985, van Staal *et al.* 1992, Lentz 1999). Peak conditions of metamorphism range from 325°C for the Caribou deposit to 425°C for Brunswick No. 12, with pressures on the order of 4 to 6 kbar (Lentz & Goodfellow 1993c, Lentz 2002, Currie *et al.* 2003); pressures were greater than 7 kbar in blueschists occurring along a D₁ thrust zone between the California Lake Group and Fournier Group (Fig. 1; van Staal *et al.* 1990). Original assemblages of sulfides and patterns of base-metal zonation are still recognizable; however, recrystallization has caused an increase in grain size of sulfide minerals, producing larger porphyroblasts of pyrite, marcasite and arsenopyrite. Sphalerite, galena and chalcopyrite exhibit linear textures due to metamorphic flow-induced deformation; pyrrhotite-rich ores exhibit a *durchbewegung* texture, an indicator of intense ductile deformation (Craig 1983, Marshall & Gilligan 1987).

Distribution of gold in massive sulfide deposits

The distribution of Au within massive sulfide deposits of the BMC is highly variable. Overall, Au displays a positive Spearman Rank correlation with Ag ($r^s =$

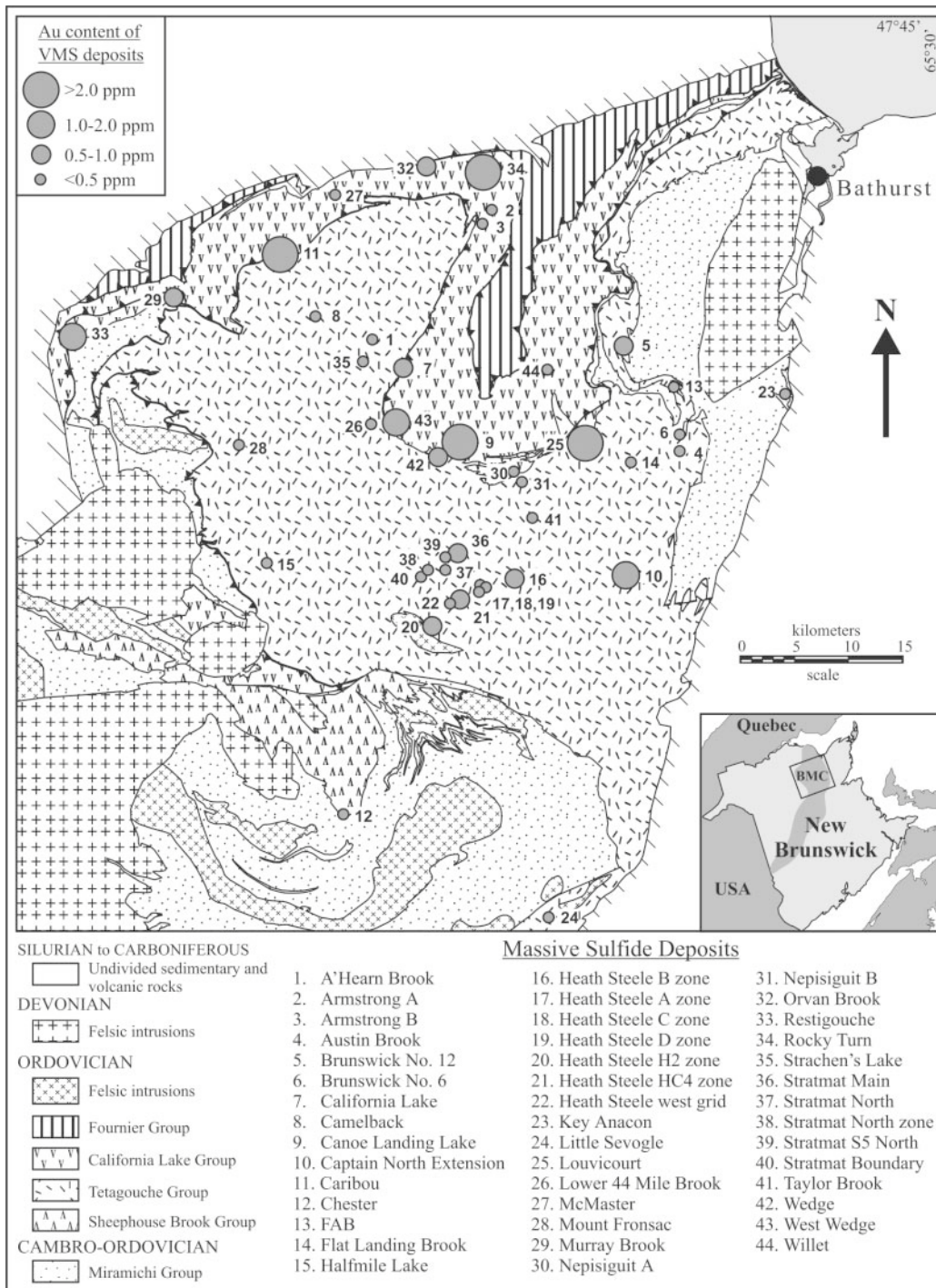


FIG. 1. Geology of the Bathurst Mining Camp (modified from McCutcheon *et al.* 2001) showing the Au content of 44 massive sulfide deposits. Gold contents were determined from the instrumental neutron-activation analysis of 215 massive sulfide samples (McClenaghan *et al.* 2003). The average Au content of the Brunswick No. 12 deposit was taken from Luff (1995). Numbers beside dots refer to deposits listed in legend.

0.53), As ($r' = 0.57$) and Sb ($r' = 0.65$, Fig. 3), but a weaker correlation with the base metals. Gold is concentrated in the feeder zone, basal sulfide and Pb- and Zn-rich lenses of massive sulfide deposits and displays

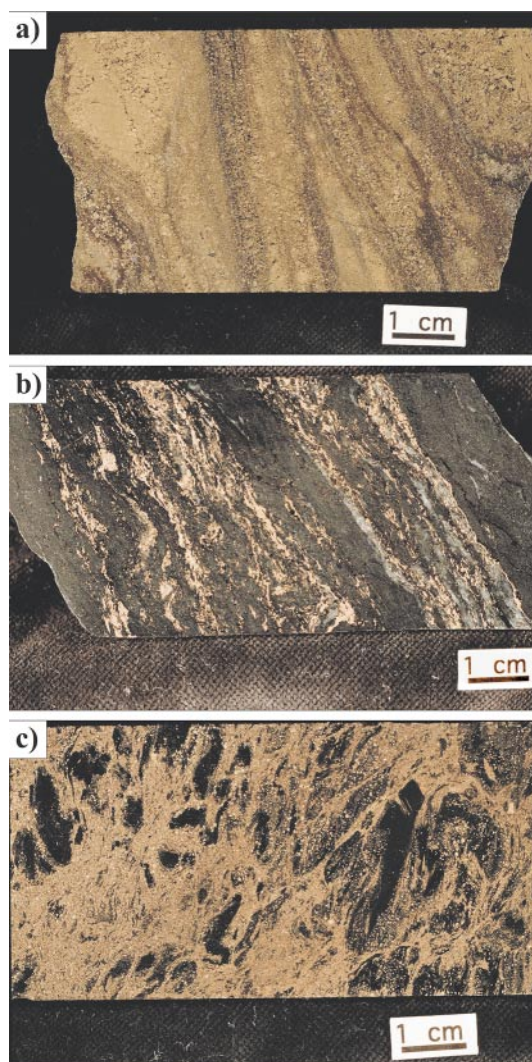


FIG. 2. Representative hand samples showing sulfide textures from massive sulfide deposits of the Bathurst Mining Camp. a) Massive banded sulfides containing pyrite, sphalerite and lesser galena from the Stratmat Main deposit. b) Siliceous veins containing pyrrhotite and minor chalcopyrite cutting hydrothermally altered (chlorite) footwall rocks in the feeder zone of the Chester deposit. Veins have been transposed parallel to the strike of the deposit owing to deformation. c) Basal sulfide facies comprised of brecciated pyrrhotite with minor pyrite and chalcopyrite in a matrix of dark green to black shale, Halfmile Lake deposit.

two distinct geochemical associations: 1) Au + Sb + As \pm Ag, and 2) Au + Bi + Co \pm Cu (McClenaghan *et al.* 2003). Basal sulfides of the Caribou deposit (Goodfellow 2003) display the Au + Bi + Co \pm Cu association, which increases in concentration toward the underlying feeder zone. Gold in Pb- and Zn-rich lenses of the Heath Steele B zone also is associated with Bi, Co and Cu, and gradually increases in concentration toward the basal sulfide facies. The Restigouche deposit displays the Au + Sb + As \pm Ag association, which is concentrated in Pb- and Zn-rich lenses that are distal with respect to the basal sulfides and feeder zone, and increases in concentration toward the hanging wall, forming a sharp zone of enrichment. The enrichment of Au toward the hanging wall is also observed in more distal portions of the Caribou deposit.

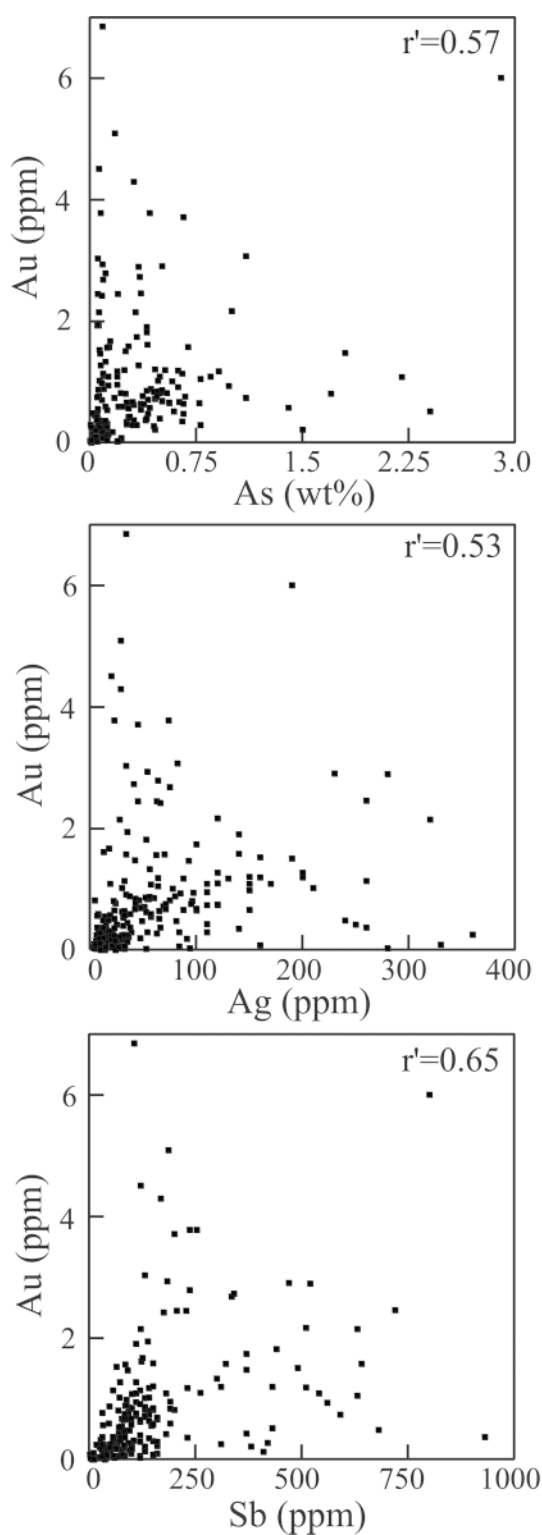
Although the basal sulfide facies of the Caribou deposit contains the highest Au grades documented in the BMC (Goodfellow 2003), Pb- and Zn-rich massive sulfides account for the greatest reservoir of Au owing to the predominance of Pb- and Zn-rich lenses, relative to other facies in massive sulfide deposits (McClenaghan *et al.* 2003).

METHODOLOGY

Sampling and bulk chemical analyses

Massive sulfide samples ($n = 215$) consisting of 50-cm portions of drill core were collected from 43 massive sulfide deposits in the Bathurst Mining Camp (Goodfellow 2003, McClenaghan *et al.* 2003). Samples and two standard reference materials, KC-1A (Abbey 1979, Bowman 1991) and MS-1 (Lentz 1995), were submitted to Activation Laboratories Ltd., ACME Laboratories Ltd. and the Geological Survey of Canada for instrumental neutron-activation analyses (INAA) and elemental analysis by inductively coupled plasma – emission spectrometry (ICP-ES) and inductively coupled plasma – mass spectrometry (ICP-MS). Results from INAA were found to be the most accurate for Au (Hannington & Gorton 1991), As, Co, Cr, Hg, Sb, Sc, Se, and W, whereas ICP-ES and ICP-MS results were used for major oxides and the remaining trace elements. Analytical results for the standard reference materials (Abbey 1979, Bowman 1991, Lentz 1995) were within acceptable limits for most of the above elements, with errors of less than 5%.

Polished thick sections of massive sulfides were prepared at the University of New Brunswick and examined under reflected light and with a scanning electron microscope (SEM). Araldite polished sections (2.5 cm in diameter) of nine sulfide samples from Au-enriched horizons in the Bathurst Mining Camp were prepared at the University of Ottawa. Sulfide textures in the nine samples were documented, and individual grains highlighted for later analyses by secondary-ion mass spectrometry (SIMS).



Micro-analytical techniques

Polished thick sections were carbon-coated and examined with a Cambridge S-200 scanning electron microscope equipped with an energy-dispersion X-ray-detection system (Link Analytical AN10 analyzer). The SEM was run at 20 kV at working distances of 24 and 25 mm, in both secondary and back-scatter modes, which provided semiquantitative determinations of the composition of the sulfide minerals.

A Cameca IMS-4f double focusing, magnetic-sector secondary-ion mass spectrometer was used to determine the Au contents of pyrite and arsenopyrite grains in massive sulfides from the Bathurst Mining Camp. Araldite sections, coated with a thin layer of carbon, were sputtered with a Cs^+ primary ion beam (50 μm raster, 10 μm diameter area of analysis), and secondary ions detected. Operating parameters for the instrument are outlined in Genkin *et al.* (1998) and McMahon & Cabri (1998). Overall, 75 SIMS analyses of pyrite in nine sections and 27 analyses of arsenopyrite in four sections were performed over three sessions. The minimum detection-level (MDL), determined from the analysis of Au-implanted standards, ranged from 532 ppb (pyrite analyses 1–36) to 452 ppb (pyrite analyses 37–75); in arsenopyrite, an MDL of 92 ppb Au was established (see Appendix). Direct-ion images of Au, As and S were acquired from a multichannel plate – fluorescent screen assembly coupled to a Photometrics Series 200 CCD camera.

Pyrite and arsenopyrite grains examined by SIMS were also analyzed for Bi, Hg, Sb, Sn, Ag, Se, As, Cu, Ni, Co, Fe and S at the University of New Brunswick using a JEOL-733 electron microprobe (Robinson *et al.* 1998). An accelerating voltage of 15 kV with a beam current of 30 nA was applied (1 μm beam) for a maximum count-time of 30 seconds.

RESULTS

The form and microscopic distribution of Au were investigated in massive sulfides from eight deposits in the BMC (Table 1). The Heath Steele B zone, Stratmat, Louvicourt, Canoe Landing Lake, Rocky Turn, Orvan

FIG. 3. Binary plots of selected elements (ICP-ES) with Au (INAA) for 215 massive sulfide samples, Bathurst Mining Camp. Overall, Au is enriched in the facies with a polymetallic Ag-As-Sb signature. A total of 132 samples are from the Heath Steele and Caribou deposits. One massive sulfide sample from the Rocky Turn deposit, which contains 3500 ppm Sb, is not plotted to better display element correlations between Au and Sb. The sample was included in the calculation of the Spearman Rank correlation coefficients displayed with each binary plot.

Brook, Murray Brook, and Restigouche deposits (Fig. 1) have bulk Au contents greater than the BMC average (0.85 ppm; McClenaghan *et al.* 2003). Native gold and Au–Ag alloy were not identified in polished sections by conventional optical and scanning electron microscopy. Furthermore, the fine-grained nature of massive sulfides in the BMC has led to difficulties in producing mineral separates for bulk analyses of pyrite, pyrrhotite, sphalerite, galena and chalcopyrite. Secondary-ion mass spec-

trometry was found to be an ideal technique, providing an analysis in an area 10 μm in diameter of pyrite and arsenopyrite grains with a low minimum detection-level.

Pyrite from the eight massive sulfide deposits was found to contain elevated Au contents (Table 2), greater than those reported by Larocque *et al.* (1995) for the Mobrun VMS deposit and by Cook & Chryssoulis (1990). SIMS analyses of pyrite yielded Au contents that range from the minimum detection-level (0.45 ppm) to 42.9 ppm (Fig. 4) and average 9.1 ppm. The frequency distribution of Au in pyrite from these deposits is positively skewed, with several overlapping populations. Owing to the small number of analyses ($n = 75$), sampling bias becomes problematic, and the distribution cannot be properly described. However, we found that euhedral grains of pyrite (Fig. 5a) contain less Au than colloform pyrite (Fig. 5c) and granular masses (Fig. 5d). Fine-grained granular pyrite most likely represents a pseudo-primary pyrite that has been recrystallized to a much smaller degree than the coarse-grained pyrite, which bears little resemblance to its original shape prior to metamorphism.

Electron-probe micro-analyses (EPMA) of pyrite from six massive sulfide deposits (Table 3) yielded low As contents for most grains, generally below the detection limit of the instrument, although pyrite from the

TABLE 1. BASE- AND PRECIOUS-METAL CONTENTS OF SAMPLES FROM EIGHT MASSIVE SULFIDE DEPOSITS, BATHURST MINING CAMP, NEW BRUNSWICK

Deposit	n	Cu wt%	Pb wt%	Zn wt%	Au ppm	Ag ppm
Canoe Landing Lake	2	0.59	0.95	3.00	2.28	47.0
Heath Steele B zone	51	1.79	1.27	3.11	0.70	69.6
Louvicourt	5	0.15	0.39	0.76	2.43	238
Murray Brook	5	0.38	2.19	3.89	0.80	40.4
Orvan Brook	4	0.69	2.18	7.00	0.90	110
Restigouche	7	0.50	4.63	7.47	1.61	96.1
Rocky Turn	1	0.26	3.30	9.40	3.07	82.0
Stratmat Main	4	0.91	5.34	13.5	1.01	118
Wedge	4	3.35	0.21	2.18	0.68	24.3

Note: Bulk sulfide samples were analyzed by INAA (Au) and ICP–ES (Cu, Pb, Zn and Ag) techniques (McClenaghan 2002).

TABLE 2. RANGE OF GOLD CONTENTS OF PYRITE OBTAINED FROM SIMS ANALYSES OF POLISHED MASSIVE SULFIDE SECTIONS, BATHURST MINING CAMP

Deposit	Hydrothermal Facies	Morphology	Min.	Avg.	Max.	n
Canoe Landing Lake	massive Py-Po-Cp	medium-grained clusters	2.1	2.4	2.7	2
		fine-grained colloform masses	11.7	15.6	19.5	2
Heath Steele B zone	fragmental Py-Po-Sp-Cp	euhedral clusters	0.7	1.1	1.3	3
		fine-grained granular mass	-	3.5	-	1
Heath Steele B zone	massive Py-Sp-Gn	granular masses	9.3	12.5	19.9	5
		medium-grained euhedral grains	<0.53	0.9	1.2	2
Louvicourt	massive Py-Sp-Gn	fine-grained granular masses	2.4	13.1	42.9	7
		coarse-grained anhedral masses	0.7	4.7	8.4	4
Murray Brook	massive Py-Sp-Gn	granular masses	6.9	18.6	32.0	11
		euhedral grain	-	0.6	-	1
Orvan Brook	massive Py-Sp-Gn	granular masses	2.2	3.9	5.6	6
		anhedral grains (100–200 μm)	<0.53	1.4	4.3	3
Restigouche	massive Py-Sp-Gn	medium-grained masses	7.6	14.1	23.7	3
		fine-grained granular masses	1.5	4.8	10.7	13
Rocky Turn	massive Py-Sp-Gn	fine-grained aggregates	16.2	23.3	31.9	4
Stratmat Main zone	massive Py-Sp-Gn	euhedral grains	2.4	3.7	4.7	3
		granular masses	2.3	3.5	5.2	4
		subhedral grain	-	0.5	-	1

Gold concentrations are quoted in ppm.

Louvicourt and Murray Brook deposits was found to be highly variable, with contents as high as 1.42 and 0.98%, respectively. Overall, variations in the As content of pyrite do not appear to correlate with the Au content of pyrite. Contents of Bi, Hg, Sb, Sn, Ag, Se, Cu and Ni in pyrite were found to be below the instrumental detection-limit (EPMA), although several grains with slightly elevated Hg values appear to coincide with elevated Au contents, possibly due to inclusions of tetrahedrite and tennantite.

Arsenopyrite grains from the Heath Steele B zone, Rocky Turn, Orvan Brook, and Murray Brook deposits were found to contain less Au than pyrite (Table 4) and much less Au than that reported by Cook & Chrissyoulis (1990) from nine deposits, worldwide. Arsenopyrite in the BMC occurs as euhedral grains (Figs. 6a, b) and as partially recrystallized clusters (Figs. 6c, d, 7a). The frequency distribution of Au in arsenopyrite (Fig. 4), determined from SIMS analyses of 27 grains, is positively skewed, with an average Au content of 2.7 ppm. Gold content ranges from 0.11 ppm for rhombohedral grains

of arsenopyrite (Fig. 6a) to 10.9 ppm Au in partially recrystallized porphyroblasts of arsenopyrite (Fig. 5b). All grains contain Au values above the detection limit for arsenopyrite (0.092 ppm). Overall, euhedral grains of arsenopyrite that formed during metamorphism have a lower Au content (avg. = 0.11 ppm) than that in partially recrystallized clusters (avg. = 10.9 ppm Au).

Twenty-five grains of arsenopyrite from four deposits (Table 5) contain between 39.9 and 43.7% As, and elevated contents of Bi, Sb and Co. Although the amount of Au does not correlate with the As content of arsenopyrite, it exhibits a positive Spearman Rank Correlation with Sb ($r' = 0.50$) and Bi ($r' = 0.54$; 95% confidence interval: $r' > 0.34$). Furthermore, an inverse correlation of Sb with Fe ($r' = -0.64$) and As ($r' = -0.45$) may indicate its incorporation into the structure. Rhombohedral grains of arsenopyrite with low Sb and Bi contents were found to contain much lower concentrations of Au than partially recrystallized clusters. Overall, the grains of arsenopyrite have low contents of Hg, Sn, Ag, Se, Cu and Ni, typically below the instrumental detection-limit (EPMA). However, a Hg-rich inclusion detected with the electron microprobe does coincide with higher Au contents in the arsenopyrite grain.

The Heath Steele B zone

Massive sulfides from the Heath Steele B zone are composed of two major facies: 1) basal fragmental sulfide composed of coarse-grained pyrite, pyrrhotite and chalcopyrite, and 2) massive pyrite with highly variable amounts of sphalerite, galena and chalcopyrite. The fragmental sulfide most likely formed as a vent-proximal facies and underwent localized brecciation and fluid-assisted sulfide infilling during the late stages of D_1 (de Roo & van Staal 2003). Texturally, the sulfides exhibit a *durchbewegung* texture (Marshall & Gilligan 1987) indicative of considerable mobilization of sulfides.

The average Au content of pyrite in a sample of coarse-grained fragmental sulfide from the Heath Steele B zone is 1.7 ppm. Gold content ranges from 0.7 ppm for medium-grained euhedral clusters to 3.5 ppm Au for a fine-grained granular mass (Table 2). The Au content of pyrite from Pb- and Zn-rich massive sulfides ranges from the detection limit (0.53 ppm) in medium-grained euhedral grains to 19.9 ppm Au in granular porphyroblasts. Overall, the average Au content of pyrite in samples examined from the Heath Steele B Zone is 9.2 ppm Au.

The Bi, Hg, Sb, Sn, Ag, Se, Cu and Ni contents of pyrite from the Heath Steele B zone are, for the most part, below the detection limit of the electron microprobe. Pyrite from the Heath Steele B zone has variable Co contents that range from the detection limit (EPMA) to 0.43%, but the amount of Co does not correlate with that of Au.

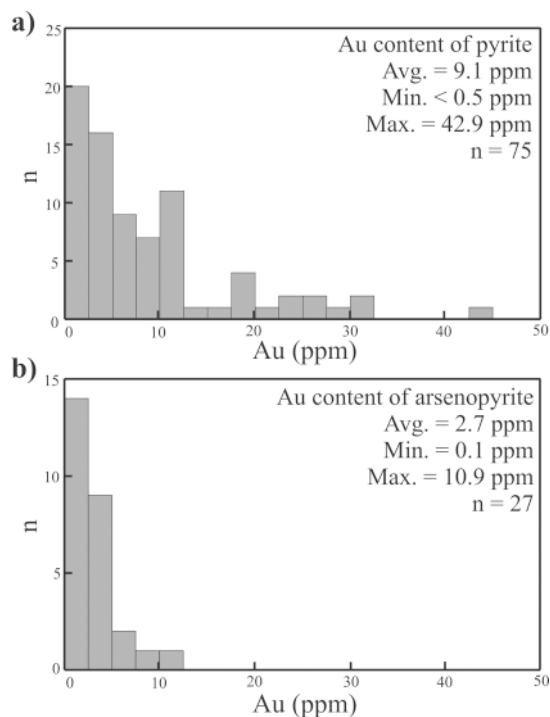


FIG. 4. Histograms showing the frequency distribution of Au in: a) 75 SIMS spot analyses of pyrite from the Heath Steele B zone, Stratmat, Canoe Landing Lake, Rocky Turn, Orvan Brook, Murray Brook, and Restigouche deposits, and b) 27 SIMS spot analyses of arsenopyrite from the Heath Steele B zone, Rocky Turn, Orvan Brook, and Murray Brook deposits.

The average Au content of fine euhedral grains of arsenopyrite (Fig. 6d) from Pb- and Zn-rich massive sulfides is 1.8 ppm, with values ranging from 0.4 to 3.1 ppm Au (Table 4).

The Louvicourt deposit

Massive sulfides from the Louvicourt deposit consist of coarse-grained pyrite with minor sphalerite and galena, and are cross-cut by late barite-rich quartz veins; tetrahedrite and native silver occur in the interstices of pyrite and barite. The average Au content of 11 grains of pyrite from the Louvicourt deposit is 10.0 ppm. The Au content averages 4.7 ppm in coarse-grained pyrite containing galena trapped along relict grain-boundaries (Fig. 6e), and 13.1 ppm in fine-grained granular masses of pyrite (Fig. 7b); the latter contain up to 42.9 ppm Au (Table 2). The As content of 11 pyrite grains from the

Louvicourt deposit ranges from the detection limit (EPMA) to 1.42% (Table 3). It does not correlate with Au, but As exhibits an inverse Spearman Rank correlation with S ($r' = -0.65$; 95% confidence interval: $r' > 0.52$). Pyrite from the Louvicourt deposit also contains elevated Bi values, which range from the detection limit of the electron microprobe to 0.43%, but do not correlate with concentrations of any other elements.

The Stratmat Main deposit

Massive pyrite, sphalerite and galena from the Stratmat Main deposit contains euhedral grains and coarse granular masses of pyrite; however, fine-grained colloform textures were not identified in the sections. Overall, the Au content of the euhedral grains and coarse granular masses of pyrite is variable at the microscopic scale, but independent of morphology. The Au contents

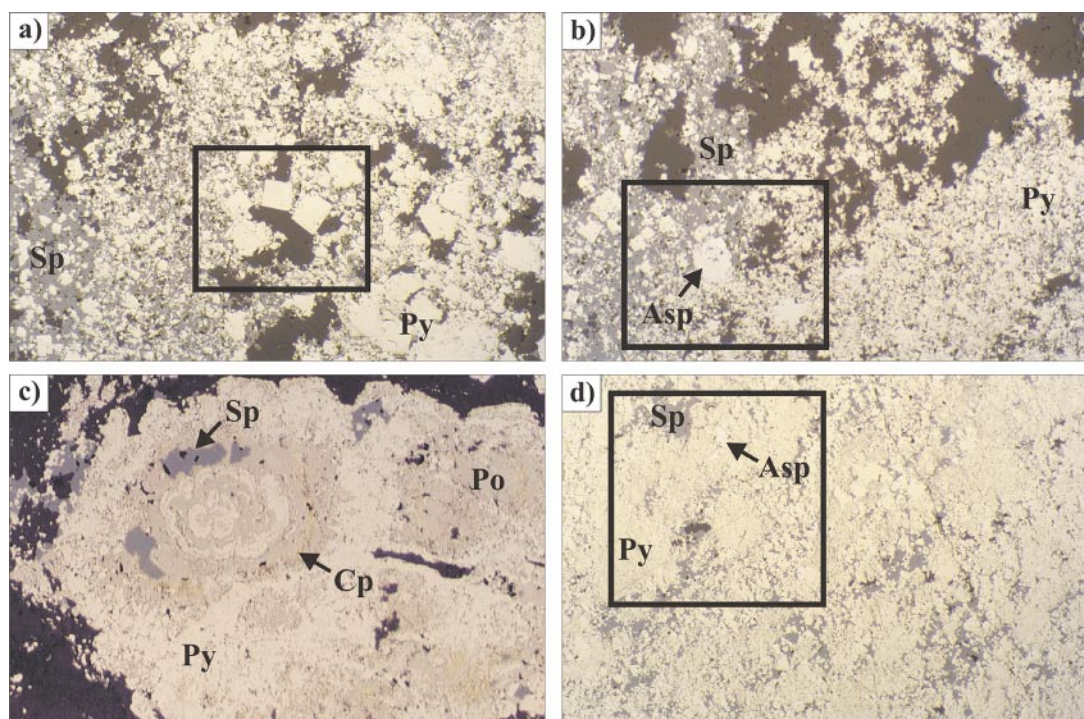


FIG. 5. Photomicrographs of massive sulfide textures observed in sections with elevated Au contents. a) Massive pyrite (yellow), and sphalerite (light grey) with quartz (dark grey), Murray Brook deposit. Note the euhedral grains of pyrite surrounded by fine-grained pyrite. The bulk Au content of the section is 1.48 ppm. Field of view is 3 mm (reflected light). b) Massive pyrite (yellow), sphalerite (light grey) and arsenopyrite (light yellow) with quartz (dark grey), Murray Brook deposit. Note the partially recrystallized clusters of arsenopyrite. Field of view is 3 mm (reflected light). c) Colloform pyrite (beige) with banding of pyrrhotite (brown), sphalerite (grey), and chalcopyrite (yellow), preserved in a matrix of chloritic sedimentary rock (black), Canoe Landing Lake deposit. The bulk Au content of the section is 2.73 ppm. Field of view is 0.4 mm (reflected light). d) Massive pyrite (yellow), sphalerite (light grey), and arsenopyrite (light yellow) with quartz (dark grey), Rocky Turn deposit. Note the fine-grained mass of pyrite and the euhedral grains of arsenopyrite. The bulk Au content of the section is 3.07 ppm. Field of view is 3 mm (reflected light).

TABLE 3. SIMS AND ELECTRON-MICROPROBE COMPOSITIONS OF PYRITE GRAINS, BATHURST MINING CAMP, NEW BRUNSWICK

Deposit	Au ppm	Bi	Sb	As	Co	Fe element %	S	Sum	Bi	Sb	As	Co	Fe atom %	S
1 Orvan Brook	2.4	<0.1	<0.06	<0.03	<0.04	46.8	54.2	101.1	0	0	0	0	33.1	66.9
2	5.0	<0.1	<0.06	0.12	0.17	46.4	53.7	100.5	0	0	0.06	0.12	33.1	66.7
3	2.6	0.15	<0.06	0.04	0.19	46.0	54.1	100.7	0.03	0	0.02	0.13	32.7	67.0
5	2.2	<0.1	<0.06	0.05	0.06	46.0	53.1	99.5	0	0	0.03	0.04	33.2	66.7
6	5.6	0.12	<0.06	<0.03	0.08	46.1	54.0	100.7	0.02	0	0	0.06	32.8	66.9
7	5.5	<0.1	<0.06	<0.03	<0.04	46.0	52.3	98.4	0	0	0	0	33.5	66.4
8	4.3	0.13	<0.06	0.14	0.08	45.7	54.5	100.6	0.02	0	0.07	0.06	32.4	67.4
9	<0.53	<0.1	<0.06	<0.03	0.05	46.8	53.9	100.9	0	0	0	0.04	33.3	66.6
10	<0.53	<0.1	<0.06	<0.03	0.08	47.1	54.1	101.5	0	0	0	0.05	33.3	66.6
28 RockyTurn	19.2	<0.1	0.22	0.16	0.06	45.7	52.1	98.7	0	0.07	0.08	0.04	33.4	66.2
29	25.9	<0.1	0.08	0.37	0.08	46.4	53.7	100.7	0	0.03	0.20	0.05	33.1	66.6
30	31.9	<0.1	<0.06	0.04	<0.04	45.0	54.3	99.4	0	0	0.02	0	32.2	67.7
31 HeathSteele	9.3	<0.1	<0.06	0.05	<0.04	46.8	52.6	99.6	0	0	0.02	0	33.7	66.2
32 Bzone	1.2	<0.1	<0.06	<0.03	0.12	46.8	52.4	99.5	0	0	0	0.08	33.8	66.0
33 Bedded	12.7	<0.1	<0.06	<0.03	0.08	46.5	51.6	98.2	0	0	0	0.05	34.1	65.8
34 Sulfide	10.6	0.12	<0.06	<0.03	0.18	47.1	52.8	100.4	0.02	0	0	0.12	33.8	66.0
35	19.9	<0.1	<0.06	<0.03	0.43	47.0	51.2	98.8	0	0	0	0.30	34.3	65.3
36	9.9	0.20	0.25	<0.03	<0.04	47.3	52.0	100.3	0.04	0.08	0	0	34.1	65.5
37	<0.53	<0.1	<0.06	<0.03	<0.04	46.8	53.0	100.0	0	0	0	0	33.7	66.3
38 Louvicourt	2.4	<0.1	<0.06	1.42	<0.04	46.1	50.4	98.2	0	0	0.78	0	34.2	65.0
39	3.3	<0.1	<0.06	0.42	0.05	46.8	50.7	98.0	0	0	0.23	0.03	34.5	65.2
40	9.8	<0.1	<0.06	0.06	0.05	47.4	51.4	99.1	0	0	0.03	0.03	34.6	65.3
41	11.7	0.43	<0.06	0.32	0.06	46.9	50.3	98.1	0.09	0	0.18	0.04	34.7	65.0
42	3.6	0.23	<0.06	0.40	0.07	46.6	51.6	98.9	0.05	0	0.22	0.05	34.0	65.7
43	6.2	0.13	<0.06	0.33	0.06	47.1	51.0	98.7	0.02	0	0.18	0.04	34.5	65.2
44	42.9	0.26	<0.06	0.74	0.05	46.0	51.0	98.7	0.05	0	0.41	0.04	33.9	65.5
45	10.4	<0.1	<0.06	0.43	0.05	47.1	50.5	98.3	0	0	0.24	0.04	34.7	64.9
46	11.0	<0.1	<0.06	<0.03	0.05	46.8	51.5	98.4	0	0	0	0.03	34.3	65.7
47	0.7	0.16	<0.06	<0.03	0.06	47.0	51.8	99.2	0.03	0	0	0.04	34.2	65.6
48	8.4	0.27	<0.06	<0.03	<0.04	47.0	52.0	99.5	0.05	0	0	0	34.1	65.8
49 MurrayBrook	6.9	0.14	<0.06	<0.03	0.05	44.9	53.7	98.8	0.03	0	0	0.03	32.4	67.5
50	10.0	<0.1	<0.06	<0.03	0.06	45.3	52.8	98.2	0	0	0	0.04	33.0	66.9
51	11.9	<0.1	0.13	0.23	0.04	45.9	53.3	99.7	0	0.04	0.12	0.03	33.0	66.8
52	24.3	0.16	<0.06	0.09	0.05	46.5	53.2	100.0	0.03	0	0.05	0.04	33.4	66.5
53	19.9	0.12	<0.06	0.82	<0.04	44.4	52.9	98.4	0.02	0	0.45	0	32.3	67.1
54	29.5	<0.1	<0.06	<0.03	0.04	46.4	53.8	100.4	0	0	0	0.03	33.1	66.8
55	27.3	<0.1	0.06	0.65	0.07	45.5	51.6	98.3	0	0.02	0.36	0.05	33.4	66.0
56	32.0	0.14	<0.06	0.12	<0.04	45.6	52.8	98.7	0.03	0	0.06	0	33.1	66.8
57	11.1	0.14	<0.06	0.31	<0.04	45.8	53.2	99.5	0.03	0	0.17	0	33.0	66.8
59	20.7	0.12	<0.06	<0.03	0.07	46.2	53.8	100.3	0.02	0	0	0.05	33.0	66.9
60	11.5	0.11	<0.06	0.98	<0.04	46.2	52.9	100.2	0.02	0	0.53	0	33.2	66.2
61	0.6	0.12	<0.06	<0.03	0.18	46.5	53.8	100.6	0.02	0	0	0.12	33.1	66.7
62 StratmatMain	3.8	<0.1	<0.06	<0.03	<0.04	46.9	52.9	100.0	0	0	0	0	33.7	66.2
63	4.7	0.14	<0.06	<0.03	<0.04	46.1	52.4	98.7	0.03	0	0	0	33.5	66.4
64	2.4	<0.1	<0.06	0.13	0.05	46.6	53.0	99.9	0	0	0.07	0.03	33.5	66.4
65	0.5	<0.1	<0.06	<0.03	0.16	47.2	52.9	100.5	0	0	0	0.11	33.8	66.0
66	5.2	0.16	<0.06	<0.03	0.04	47.3	52.7	100.4	0.03	0	0	0.03	34.0	65.9
67	2.3	0.14	<0.06	0.07	0.27	47.1	52.7	100.6	0.03	0	0.04	0.19	33.8	65.8
68	3.0	0.13	<0.06	<0.03	0.04	47.1	52.7	100.0	0.03	0	0	0.03	33.9	66.0
69	3.7	<0.1	0.22	0.06	<0.04	47.0	52.9	100.6	0	0.07	0.03	0	33.7	66.0

Note: Gold concentration obtained on a Cameca IMS-4f secondary-ion mass spectrometer (SIMS) at the Canada Centre for Mineral and Energy Technology. Remaining analyses were made using a JEOL-733 electron microprobe at the University of New Brunswick.

of pyrite range from 0.48 to 5.2 ppm (Table 2) and average 3.2 ppm Au. Trace-element contents are low in eight grains of pyrite from the Stratmat Main deposit, and do not exhibit any significant correlations. Arsenic contents are also low, ranging from the detection limit (EPMA) to 0.13% (Table 3).

The Canoe Landing Lake deposit

Massive sulfides from the Canoe Landing Lake deposit consist of fine- to coarse-grained pyrite, pyrrhotite, sphalerite, and galena with minor chalcopyrite.

TABLE 4. RANGE OF GOLD CONTENTS OF ARSENOPYRITE OBTAINED FROM SIMS ANALYSES OF POLISHED MASSIVE SULFIDE SECTIONS, BATHURST MINING CAMP

Deposit	Hydrothermal Facies	Morphology	Min.	Avg.	Max.	n
Heath Steele B zone	massive Py-Sp-Gn	fine-grained, rhombohedral grains	0.4	1.8	3.1	3
Murray Brook	massive Py-Sp-Gn	rhombohedral grains and clusters	1.4	4.4	10.9	6
Orvan Brook	massive Py-Sp-Gn	granular masses (~150 µm)	2.2	4.6	9.4	7
		granular masses (~800 µm)	2.5	2.9	3.3	4
Rocky Turn	massive Py-Sp-Gn	rhombohedral grains and clusters	0.1	0.2	0.3	7

Gold concentrations are quoted in ppm.

TABLE 5. SIMS AND ELECTRON-MICROPROBE COMPOSITIONS OF ARSENOPYRITE GRAINS, BATHURST MINING CAMP, NEW BRUNSWICK

Deposit	Au ppm	Bi	Sb	As	Co	Fe	S	Sum	Bi	Sb	As	Co	Fe	S
				element %							atom %			
1 Rocky Turn	0.2	<0.1	<0.06	40.9	0.05	35.6	22.0	98.7	0	0	29.2	0.04	34.0	36.7
	0.3	<0.1	<0.06	42.5	<0.04	35.1	20.6	98.4	0	0	30.8	0	34.1	34.9
	0.2	<0.1	0.12	42.2	<0.04	36.0	20.7	99.2	0	0.05	30.3	0	34.8	34.7
	0.2	<0.1	0.16	40.6	0.14	35.8	20.8	97.8	0	0.07	29.5	0.13	34.8	35.3
	0.1	<0.1	0.10	41.9	0.56	36.2	20.9	100.1	0	0.04	29.8	0.51	34.6	34.9
	0.1	<0.1	<0.06	42.0	<0.04	36.0	20.8	98.9	0	0	30.2	0	34.8	34.9
	0.1	<0.1	<0.06	42.3	0.06	35.4	20.7	98.6	0	0	30.6	0.05	34.4	35.0
8 Orvan Brook	3.7	0.25	1.33	41.2	0.16	34.7	20.7	98.4	0.07	0.59	30.0	0.15	33.9	35.3
	2.2	0.23	3.15	39.3	0.19	34.6	20.4	97.9	0.06	1.43	29.0	0.18	34.2	35.1
	5.0	0.19	3.61	40.0	0.05	33.3	20.1	97.4	0.05	1.65	29.8	0.04	33.3	35.1
	9.4	<0.1	0.31	42.4	0.24	35.5	20.5	98.9	0	0.14	30.6	0.22	34.4	34.6
	4.7	0.15	0.83	42.2	0.43	35.0	20.0	98.6	0.04	0.37	30.8	0.40	34.3	34.1
	3.3	0.54	1.47	41.1	0.14	35.1	20.6	99.0	0.14	0.66	29.8	0.13	34.3	34.9
	2.5	0.49	1.83	40.9	0.30	34.7	20.2	98.4	0.13	0.83	30.0	0.28	34.2	34.6
	3.0	0.27	2.10	41.6	0.62	34.9	19.6	99.2	0.07	0.95	30.5	0.58	34.3	33.6
	3.0	<0.1	1.60	42.0	0.04	35.2	20.2	99.2	0	0.72	30.5	0.04	34.3	34.4
	4.3	<0.1	0.83	42.1	0.53	34.4	20.4	98.5	0	0.37	30.7	0.49	33.7	34.7
19 Heath Steele 20 B zone 21 Bedded Sulfide	1.7	<0.1	0.76	42.4	0.76	35.5	19.9	99.5	0	0.34	30.7	0.70	34.5	33.7
	0.4	<0.1	1.23	41.4	0.76	34.7	19.8	97.9	0	0.56	30.5	0.71	34.2	34.0
	3.1	0.46	1.78	41.6	3.40	32.5	19.6	99.9	0.12	0.80	30.4	3.16	31.9	33.4
22 Murray Brook 23 24 25 26 27	5.4	0.16	0.65	42.8	0.05	34.6	19.4	97.7	0.04	0.30	31.7	0.05	34.4	33.5
	10.9	0.36	0.89	43.0	0.19	34.7	19.8	99.1	0.10	0.40	31.4	0.18	34.0	33.9
	4.9	0.15	0.39	43.7	0.45	33.4	19.4	97.5	0.04	0.18	32.5	0.43	33.3	33.6
	2.2	0.45	0.66	41.6	0.17	35.2	19.9	98.0	0.12	0.30	30.6	0.16	34.7	34.1
	1.4	0.14	0.93	42.9	0.08	35.1	19.0	98.2	0.04	0.42	31.8	0.07	34.8	32.9
	1.4	<0.1	0.99	40.3	<0.04	35.1	20.3	96.8	0	0.45	29.8	0	34.7	35.0

Note: Gold concentration obtained on a Cameca IMS-4f secondary-ion mass spectrometer (SIMS) at the Canada Centre for Mineral and Energy Technology. Remaining analyses were made using a JEOL-733 electron-microprobe at the University of New Brunswick.

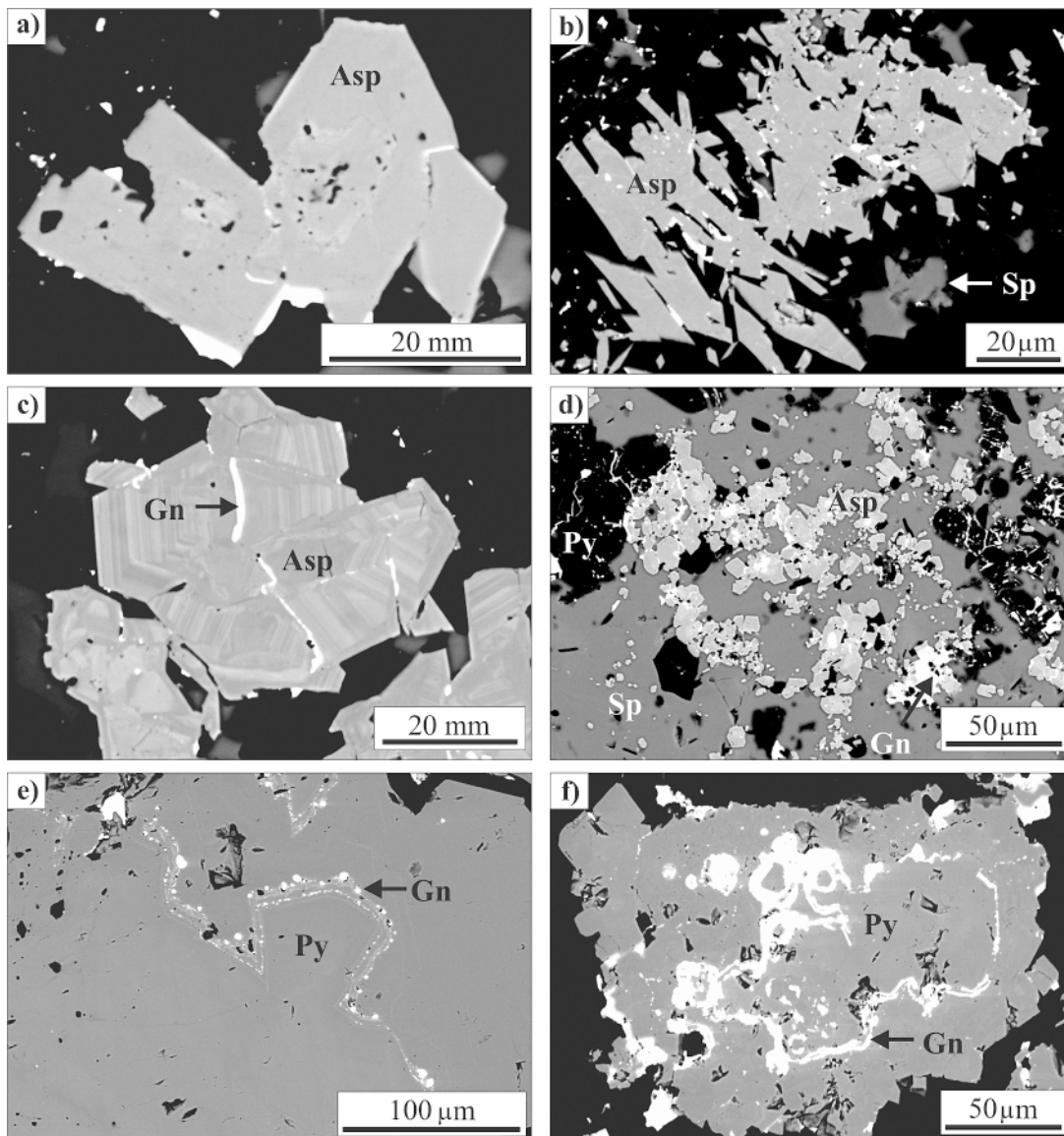


FIG. 6. Back-scattered electron images of sulfides from sections containing elevated Au contents. a) Grains of hexagonal and rhombohedral arsenopyrite (grey) surrounded by fine-grained pyrite (black) and sphalerite (dark grey), Rocky Turn deposit. The average Au content of arsenopyrite in the section is 0.2 ppm. b) An aggregate of rhombohedral arsenopyrite grains (grey) with inclusions of galena (white) and surrounded by fine-grained pyrite (black) and sphalerite (dark grey), Murray Brook deposit. The average Au content of arsenopyrite in the section is 4.4 ppm. c) A cluster of recrystallized hexagonal arsenopyrite grains (grey) surrounded by fine-grained pyrite (black) and sphalerite (dark grey), Orvan Brook deposit. The arsenopyrite grains display concentric zonation with respect to arsenic. The average Au content of arsenopyrite in the section is 2.9 ppm. d) Clusters of grains of hexagonal and rhombohedral arsenopyrite (grey) surrounded by sphalerite (dark grey), galena (white), and pyrite (black), Heath Steele B zone. The average Au content of arsenopyrite in the section is 1.8 ppm. e) Coarse-grained recrystallized pyrite (grey) marked by relict grain boundaries that contain inclusions of galena, Louvicourt deposit. The average Au content of coarse-grained pyrite from the deposit is 4.7 ppm. f) A partially recrystallized mass of pyrite (grey) containing interstitial galena (white) and surrounded by sphalerite (black), Restigouche deposit. The average Au content of pyrite in the section is 14.1 ppm.

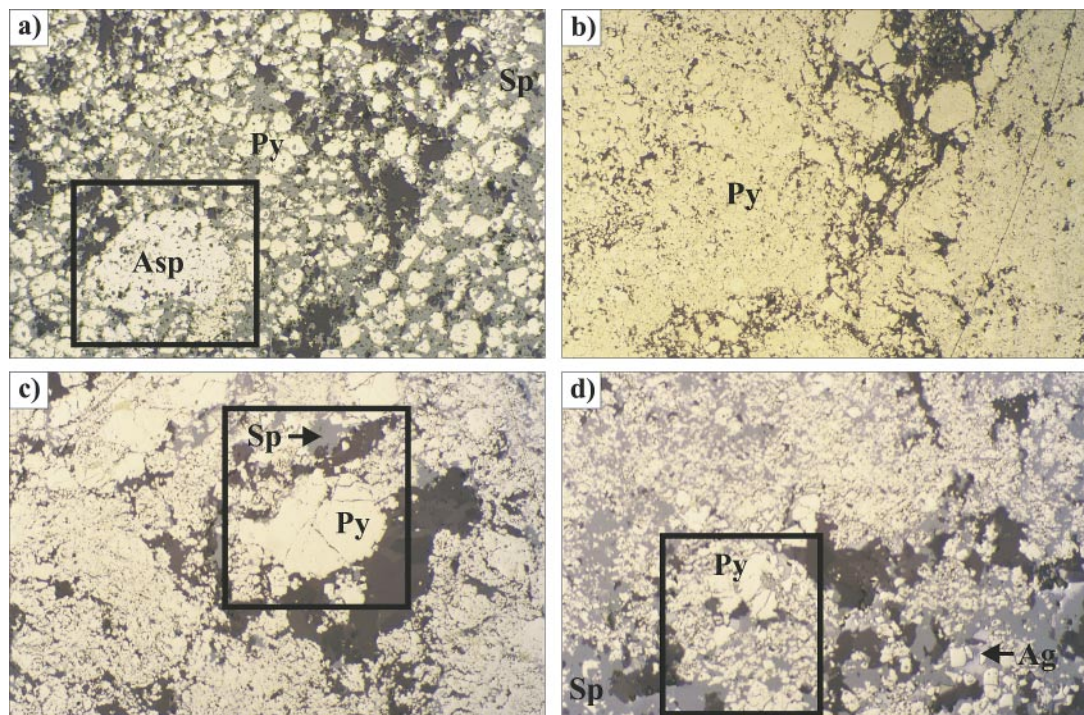


FIG. 7. Photomicrographs of massive sulfide textures in sections with elevated Au contents (reflected light). a) Massive pyrite (yellow), arsenopyrite (light yellow) and sphalerite (light grey) with quartz (dark grey), Orvan Brook deposit. Note the granular mass of arsenopyrite and the anhedral grains of pyrite found throughout the section. The bulk Au content of the sulfide section is 1.18 ppm. Field of view is 3 mm. b) Fine-grained granular pyrite (yellow) in a groundmass of quartz and barite (dark grey), Louvicourt deposit. The bulk Au content of the section is 2.91 ppm. Field of view is 3 mm. c) Massive pyrite (light yellow), sphalerite (light grey), and chalcopyrite (yellow) with quartz (dark grey), Restigouche deposit. Note the medium- to coarse-grained recrystallized pyrite with triple junctions and the surrounding fine-grained granular pyrite. The bulk average Au content of the section is 6.01 ppm. Field of view is 3 mm. d) Massive pyrite (yellow), sphalerite (light grey) and native silver (greenish grey) with quartz (dark grey), Restigouche deposit. Note the cluster of spheroidal pyrite grains. Field of view is 3 mm.

Pyrrhotite and chalcopyrite fill dilatant fractures in pyrite, and form a fine-grained matrix with sphalerite, which occurs in the interstices of pyrite and arsenopyrite. Pyrite displays a wide range of textures, including spheroidal and colloform masses (Fig. 5c) and medium-grained clusters. The average Au content of pyrite in the samples analyzed is 9.0 ppm, and Au content ranges from 2.1 ppm for medium-grained clusters to 19.5 ppm Au for colloform and spheroidal forms (Table 2). Arsenopyrite (not analyzed with SIMS) occurs as clusters and wispy bands that traverse the section.

The Rocky Turn deposit

Sulfides from the Rocky Turn deposit consist of fine- to medium-grained pyrite, sphalerite, and galena, with minor arsenopyrite. Four analyses of fine-grained masses of pyrite (Fig. 5d) yielded an average Au con-

tent of 23.3 ppm, with a maximum content of 31.9 ppm Au. Despite the high contents of Au, the As content was found to be low, ranging from 0.04 to 0.37% As in three pyrite grains, and does not covary with Au.

Arsenopyrite, also present within fine-grained pyrite and sphalerite, forms euhedral grains (30 μm in size) and clusters (Fig. 6a). The Au content of seven grains of arsenopyrite from the Rocky Turn deposit is the lowest measured in the BMC, with 0.18 ppm Au, on average (Table 4), and coincides with very low Sb contents that range from the detection limit (EPMA) to 0.16% (Table 5). The average Sb content of arsenopyrite for the remaining deposits examined is 1.33%. Arsenic exhibits an inverse Spearman Rank correlation with S ($r' = -0.86$; 95% confidence interval: $r' > 0.67$); however, the Au content does not correlate with any of the elements quoted

The Orvan Brook deposit

Massive sulfides from the Orvan Brook deposit consist of fine- to coarse-grained pyrite with interstitial quartz, sphalerite, galena and chalcopyrite. Pyrite occurs as fine-grained spheroidal (Fig. 7a) and subhedral grains, and has an overall mottled appearance. The Au content of pyrite ranges from the detection limit (0.53 ppm) for anhedral grains to 5.6 ppm Au in granular masses (Table 2), and has an average Au content of 3.16 ppm. Overall, trace-element contents of nine grains of pyrite from the Orvan Brook deposit are variable and generally below the detection limit of the electron microprobe (Table 3).

Arsenopyrite occurs as large clusters of partially recrystallized grains (Fig. 7a); they are compositionally zoned with respect to arsenic (Fig. 6c). The Au content of 11 grains of arsenopyrite from the Orvan Brook deposit ranges from 2.2 to 9.4 ppm (Table 4), with an average of 4.0 ppm Au. Six SIMS spot analyses of sphalerite yielded one result above detection, with a Au content of 0.3 ppm.

The Sb content of 10 arsenopyrite grains ranges from 0.31 to 3.61% Sb and exhibits an inverse Spearman Rank correlation with As ($r' = -0.86$; 95% confidence interval: $r' > 0.55$). The arsenopyrite from Orvan Brook has the highest Bi contents of the deposits analyzed, reaching values of 0.54%. The Hg, Sn, Ag, Se, Cu and Ni contents of arsenopyrite are below the detection limit of the electron microprobe (Table 5).

The Murray Brook deposit

Sulfides from the Murray Brook deposit are composed of medium- to coarse-grained pyrite interbedded with sphalerite and chalcopyrite within a siliceous matrix. Pyrite forms euhedral grains, and granular and spheroidal masses. The Au content of 12 grains of pyrite from the Murray Brook deposit ranges from 0.6 ppm in one euhedral grain (Fig. 5a) to 32.0 ppm in granular masses (Table 2), with an average of 17.1 ppm Au. The As content ranges from the detection limit (EPMA) to 0.98% and does not covary with the Au content of pyrite. The remaining trace-element contents of pyrite are near or below the detection limit of the electron microprobe (Table 3).

Arsenopyrite occurs as rhombohedral grains and wispy bands in anhedral clusters of pyrite grains. The Au content of arsenopyrite from the Murray Brook deposit ranges from 1.4 ppm in euhedral grains (Fig. 6b) to 10.9 ppm in partially recrystallized clusters (Fig. 5d), averaging 4.4 ppm Au (Table 4). Six grains of arsenopyrite were found to contain elevated Bi, Sb and Co contents, whereas Hg, Sn, Ag, Se, Cu and Ni were found to be below detection (EPMA). The Sb contents of arsenopyrite are lower than those from the Heath Steele B zone and Orvan Brook deposits, averaging 0.75%. How-

ever, As contents are the highest, averaging 42.4%, which exhibits a positive Spearman Rank correlation with Co ($r' = 0.83$; 95% confidence interval: $r' > 0.73$). Sphalerite also was found to contain trace amounts of Au, ranging from 0.21 to 0.24 ppm for two SIMS analyses.

The Restigouche deposit

Massive sulfides from the Restigouche deposit consist of fine- to medium-grained pyrite with interstitial sphalerite, galena, chalcopyrite and pyrrhotite in a siliceous groundmass (Fig. 7c). Despite bulk contents of up to 3 wt% As in several samples, arsenopyrite was not identified by conventional microscopy. The Au content of 16 grains of pyrite ranges from 1.5 ppm in fine-grained granular masses to 23.7 ppm in medium-grained layers composed of partially recrystallized pyrite (Fig. 7c) and spheroidal grains (Fig. 7d), and averages 6.5 ppm Au.

The distribution of gold in pyrite and arsenopyrite

The abundance, distribution and morphology of sub-microscopic Au, which may include nanometric inclusions or chemically bonded Au in the sulfide structure (Cabri *et al.* 1989, Wagner *et al.* 1986) may be elucidated with sensitive ^{197}Au ion imaging. Ion images of arsenopyrite in massive sulfides from the Murray Brook deposit (Fig. 8) display the elemental distribution of As (blue) and Au (red-magenta); the intensity of the red color in Figure 8 increases with an increased Au content. Spot areas, displaying an intense magenta color with well-defined boundaries, indicate the presence of Au-rich inclusions. The purple to light pink color corresponds to fine-grained Au occurring either as sub-microscopic inclusions beyond the resolution of the ion-microprobe or as chemically bonded Au in the sulfide structure. The distribution of fine-grained Au can be described as homogeneous or heterogeneous and is discriminated by variations in color. Gold is heterogeneously distributed as a fine-grained fraction and as Au-rich inclusions along the edges of rhombohedral grains (Fig. 8a) and recrystallized clusters (Figs. 8b, c) of arsenopyrite.

Images of pyrite from the Murray Brook deposit (Figs. 9b, d) based on the ^{197}Au ion display highly variable Au and As contents, which are heterogeneously distributed throughout partially recrystallized masses. A fine-grained Au fraction also occurs throughout grains of pyrite, whereas Au-rich inclusions (alloy) are concentrated along edges of As-rich patches (Fig. 9d).

Coarse-grained masses of pyrite from the Restigouche deposit also contain variable Au and As contents (Figs. 10b, d). Recrystallization has led to the juxtaposition of grains devoid of As and Au (black in Fig. 10d) with grains containing higher Au contents.

Gold is heterogeneously distributed (Fig. 10d) in pyrite with high As contents; Au-rich inclusions also occur near As-rich zones in pyrite.

DISCUSSION

The occurrence of gold

The micro-analytical results and an overall positive Spearman Rank Au correlation with As (Fig. 3) suggest that pyrite in the BMC is arsenian (Sutherland 1967) and the principal host of gold in the massive sulfides. However, on the scale of individual grains of pyrite, a weak Spearman Rank correlation exists between Au and As. The weak correlation is most likely a result of highly variable intra-granular As contents, as seen in ion images of pyrite (Figs. 9, 10) and inconsistent results of electron-probe micro-analyses (Table 3). Arsenian pyrite in the BMC is restricted to low As contents, and does not extend toward end-member arsenopyrite (FeAsS) compositions, resulting in pyrite and arsenopyrite populations that are distinct with respect to their As and S contents (Fig. 11a).

Arsenopyrite, which contains lower Au contents, is not as prevalent as pyrite in massive sulfides and contributes less to the overall gold-distribution budget of the BMC. Although the Brunswick No. 12 deposit was not sampled as part of this study, LeBlanc (1989) and Chryssoulis & Agha (1990) found that Au at Brunswick No. 12 occurs as a Au–Ag alloy, native Au, and refractory Au in pyrite and arsenopyrite. Roughly 60% of the total assayed Au was attributed to “invisible Au”, using the terminology of Bürg (1930) and Boyle (1979) in pyrite and arsenopyrite. The remaining 40% of the Au at Brunswick No. 12 was attributed to native Au and two forms of a Au–Ag alloy (LeBlanc 1989).

Submicroscopic Au can occur in a chemically bonded form in the structures of pyrite and arsenopyrite (Cabri *et al.* 1989, Cook & Chryssoulis 1990), or as discrete inclusions, which are undetectable by conventional electron-microprobe techniques (Chryssoulis *et al.*

1989). An inverse Spearman Rank correlation between As and S ($r' = -0.75$; Fig. 11b) is consistent with As substitution for S in arsenopyrite (Fleet *et al.* 1989). A positive Spearman Rank correlation between Au and Sb ($r' = 0.50$), and inverse correlations between Au and Fe ($r' = -0.66$; Fig. 12) and Sb and Fe ($r' = -0.64$), suggest incorporation of Au and Sb in place of Fe in the arse-

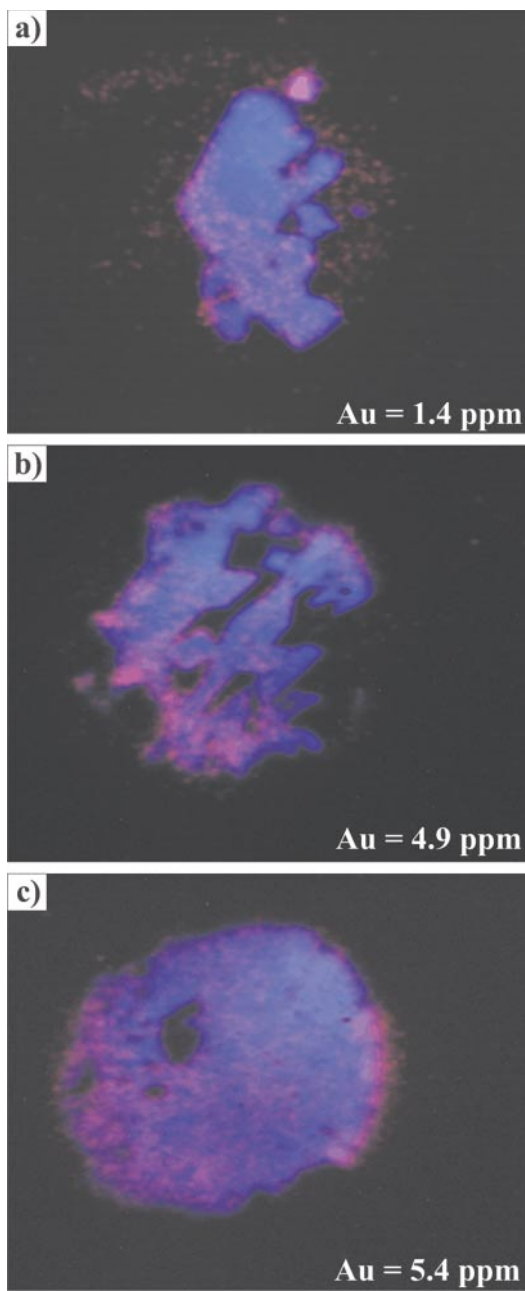


FIG. 8. Direct-ion SIMS images of arsenopyrite from the Murray Brook massive sulfide deposit. Field of view is 62.5 μm . a) SIMS image overlay of Au (red-magenta) and As (blue) images for rhombohedral arsenopyrite grains containing 1.4 ppm Au. Gold occurs as a fine-grained disseminated fraction that is concentrated along grain edges and as a Au-rich inclusion. b) SIMS image overlay of a cluster of euhedral grains of arsenopyrite containing 4.95 ppm Au. Gold is concentrated toward the edges of arsenopyrite grains and clusters. c) SIMS image overlay of a granular cluster of arsenopyrite containing 5.4 ppm. Gold is heterogeneously distributed throughout the grain and is concentrated along its edges.

nopyrite structure, possibly in the form of aurostibite (AuSb_2).

Additional species that may host Au include chalcopyrite, pyrrhotite, sphalerite, tennantite and tetrahedrite. Limited analyses of sphalerite in this study indicate that it does not contain large amounts of Au, typically less than 0.3 ppm. Similarly, pyrrhotite does not generally contain appreciable amounts of gold, with contents only reaching a maximum of 0.03–0.06 ppm Au at the Mobrún deposit in northwestern Quebec (Larocque *et al.* 1995). Larocque *et al.* also reported Au contents reaching a maximum in the 0.5–1 ppm range for chalcopyrite, and likewise chalcopyrite may contribute to the Au content of some deposits in the BMC. However, owing to the preponderance of pyrite in massive sulfides of the BMC, pyrite will account for the bulk of the mineralogical distribution of Au.

The syngenetic deposition of gold

Huston *et al.* (1992) have suggested that the mineralogy and grain size of Au-bearing phases in massive sulfide deposits of eastern Australia may be controlled in part by constraints governing hydrothermal transport of Au. Similar to the volcanic-rock-hosted deposits of eastern Australia (Huston & Large 1989), the association of Au in the BMC with two different suites of elements, $\text{Au} + \text{Sb} + \text{As} \pm \text{Ag}$ and $\text{Au} + \text{Bi} + \text{Co} \pm \text{Cu}$, has been attributed to evolving conditions of the hydrothermal fluid, specifically Au transport and deposition between the high-temperature proximal and the lower-temperature distal portions of the massive sulfide deposits (McClenaghan *et al.* 2003).

The presence of a pyrite – pyrrhotite – chalcopyrite assemblage, common in the stringer sulfides underlying

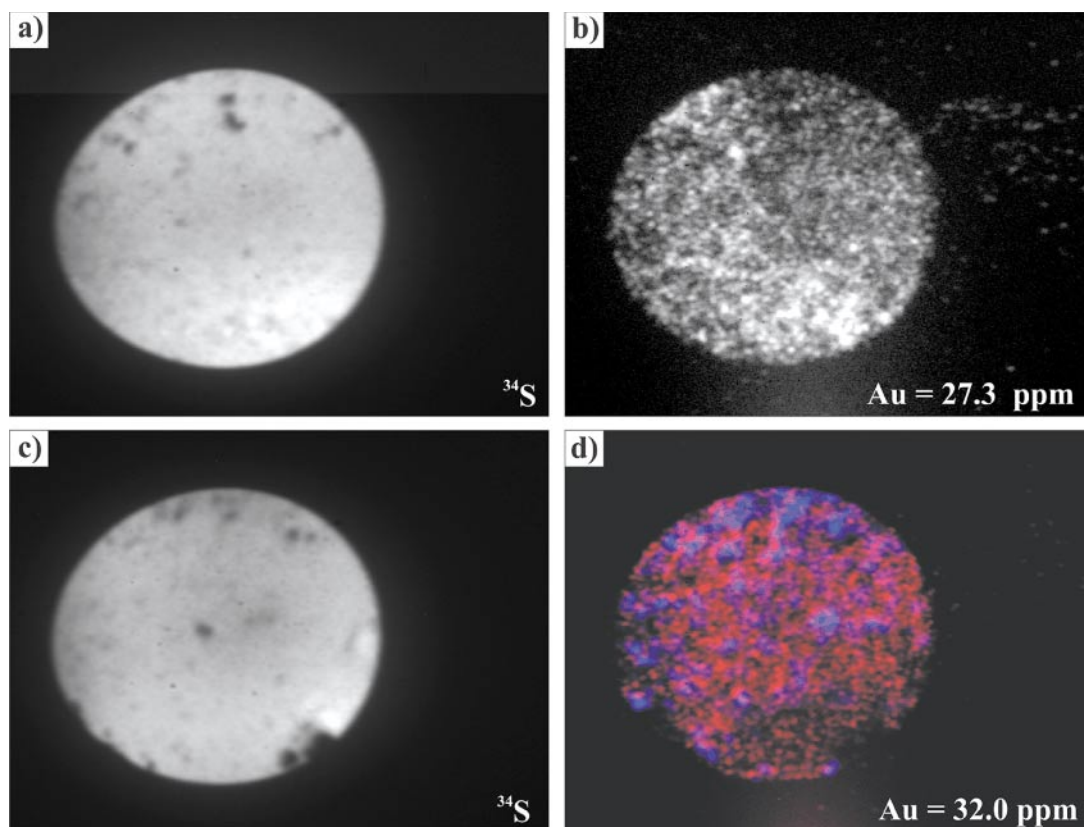


FIG. 9. Direct-ion SIMS images of pyrite from the Murray Brook massive sulfide deposit. Field of view is 100 μm . a) SIMS image showing the distribution of ^{34}S throughout a fine-grained granular mass of pyrite containing 27.3 ppm Au. b) SIMS image displaying a fine-grained fraction of Au (light grey background) with Au-rich inclusions (white). c) SIMS image of ^{34}S throughout a medium-grained granular mass of pyrite containing 32.0 ppm Au. d) SIMS image overlay of Au (red-magenta) and As (blue) images displaying the distribution of a fine-grained fraction of Au accompanied by Au-rich inclusions surrounding As-rich regions.

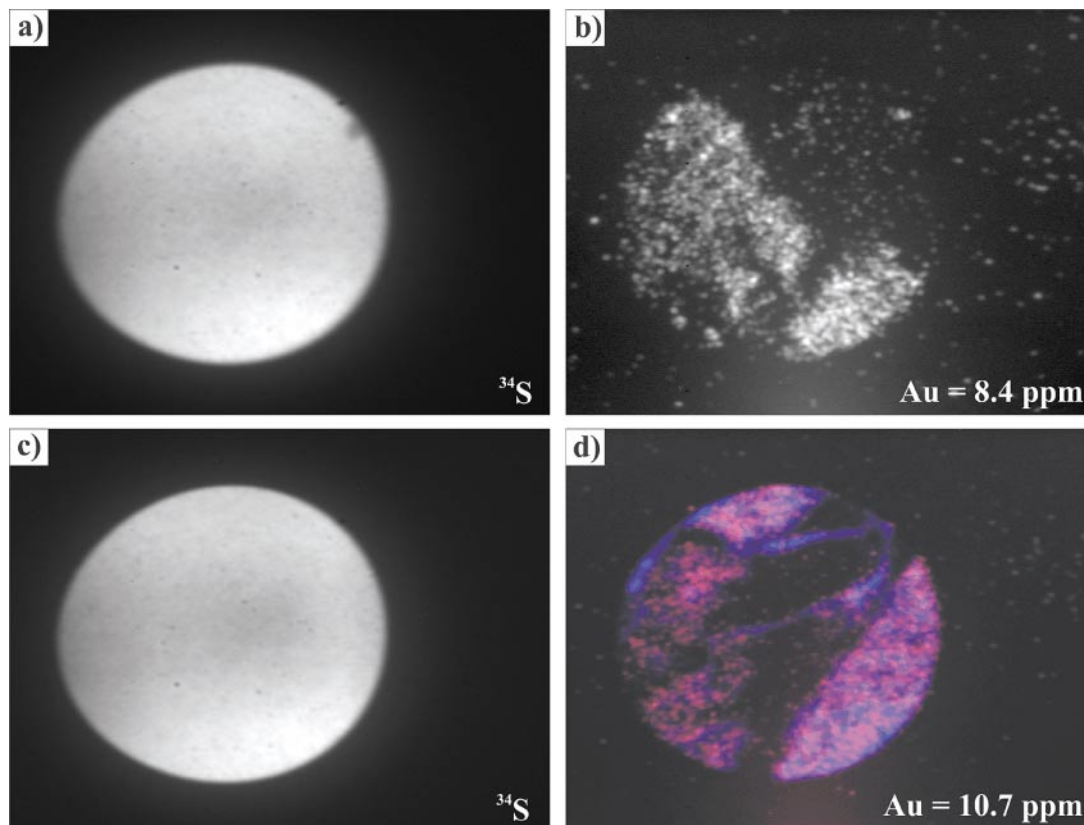


FIG. 10. Direct-ion SIMS images of pyrite from the Restigouche massive sulfide deposit. Field of view is $62.5 \mu\text{m}$. a) SIMS image showing the homogeneous distribution of ^{34}S throughout a coarse-grained recrystallized mass of pyrite containing 8.4 ppm Au. b) SIMS image of Au (grey) for coarse-grained pyrite displaying a heterogeneous distribution of Au as a fine-grained fraction (grey) and Au-rich inclusions (white). c) SIMS image of ^{34}S throughout coarse-grained recrystallized pyrite, highlighted in Figure 7c. d) SIMS image overlay of Au (red-magenta) and As (blue) images for the coarse-grained recrystallized pyrite. Gold is heterogeneously distributed and is enriched in the As-rich portions of the grain.

ing many deposits in the Bathurst Mining Camp, means that fluids were fairly reduced, with temperatures at the base of these deposits exceeding 300°C (Lentz & Goodfellow 1993a, b). Stringer veins in the feeder zone can contain fine-grained skeletal pyrite–arsenopyrite intergrowths, delicately zoned owing to variable metamorphic re-equilibration with host assemblages. This re-equilibration has resulted in the liberation of As from the outer rim of arsenopyrite grains and a low As/S value (Lentz 2002). The cores of these grains do not contain any inclusions and have not re-equilibrated to a lower As contents during metamorphism. The higher ratio of As (31.5 to 33.4 atom % As; Lentz 2002) to sulfur is interpreted to reflect primary compositions of arsenopyrite (Lentz 2002). Saturation of arsenopyrite with these high As contents would occur between 350° and 450°C (Kretschmar & Scott 1976), provided a low $a_{\text{H}_2\text{S}}$ is maintained.

Under these relatively high-temperature conditions, Au transport in hydrothermal fluids will be dominated by the AuCl_2^- and $\text{Au}(\text{HS})^0$ complexes. The mixing of hydrothermal fluids with seawater would have led to an increase in pH and $f(\text{O}_2)$, and a decrease in temperature and $a(\text{H}_2\text{S})$, resulting in the deposition of Au and Ag as an alloy in a primitive bedded sulfide facies. Zone refining of massive sulfides (Large 1977, Pisutha-Arnond & Ohmoto 1983) led to the subsequent redistribution of Au, initially deposited within the primitive bedded sulfide facies. Within the core of the basal sulfide facies, an increase in pH accompanying the replacement of pyrite, sphalerite and galena by chalcopyrite likely resulted in the precipitation of Au from the AuCl_2^- complex (Huston & Large 1989).

At the Brunswick No. 12 deposit, a Au-rich alloy ($\text{Au}_{91}\text{Ag}_9$) occurs in proximal high-temperature stockwork veins of pyrite and pyrrotite (LeBlanc

1989). The deficiency of Ag in this alloy may be a result of the increased stability of the AgCl_2^- complex at elevated temperatures (Hannington & Scott 1989), relative to AuCl_2^- . The lack of native Au may be due to an increased $a(\text{H}_2\text{S})$ (Shikazono & Shimizu 1987, Gammons & Williams-Jones 1995) as well as elevated temperatures and lower pH (Hannington & Scott 1989, Huston *et al.* 1992).

A Ag-rich alloy ($\text{Au}_{49}\text{Ag}_{51}$) occurs in distal lenses of pyritic chert, indicating simultaneous destabilization of both the AgCl_2^- and AuCl_2^- complexes, likely owing to a decrease in $a(\text{H}_2\text{S})$ and temperature, and an increase in pH accompanying the mixing of hydrothermal fluids with seawater.

Gold is also remobilized toward the top of the sulfide bodies as the $\text{Au}(\text{HS})_2^-$ complex (Hannington *et al.* 1986) and deposited along with Sb, As and Ag near the seafloor due to a decrease in temperature and $a(\text{H}_2\text{S})$, and an increase in pH and $f(\text{O}_2)$. A decrease in $a(\text{H}_2\text{S})$ through the precipitation of pyrite would result in the deposition of Au as a submicroscopic fraction in Fe-sulfides (Healy & Petruk 1990). The arsenian nature of pyrite in the BMC is due to trace arsenic substitution for sulfur in pyrite as $[\text{AsS}]^{3-}$ or As_2 . This results in an overall imbalance in charges, promoting the incorporation of trivalent cations of Au, As and Sb (Cook & Chryssoulis 1990), as indicated by the positive Spearman Rank correlations between Au, Sb and As.

Post-depositional effects

Variable amounts of recrystallization have generated pyrite and arsenopyrite that contain lower Au contents than less recrystallized grains. Within pseudo-primary pyrite, Au occurs in a chemically bonded form and as Au-rich inclusions surrounding As-rich patches in py-

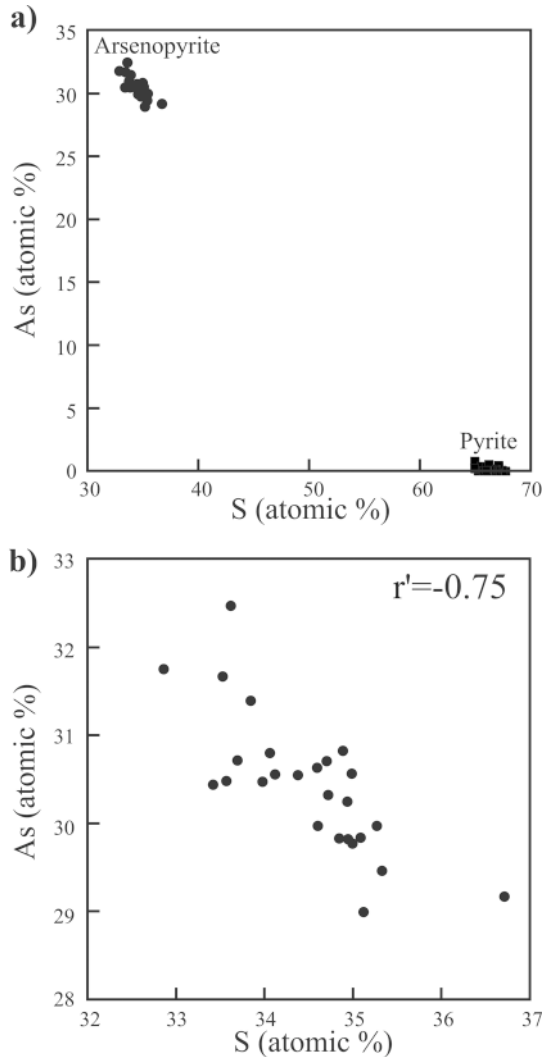


FIG. 11. Electron-microprobe compositions of pyrite (■) and arsenopyrite (●) from the Bathurst Mining Camp. a) Pyrite exhibits a narrow range of As contents indicating limited substitution of As in pyrite throughout the Bathurst Mining Camp. b) The As content of 26 arsenopyrite grains is highly variable and exhibits an inverse Spearman Rank correlation with S ($r' = -0.75$).

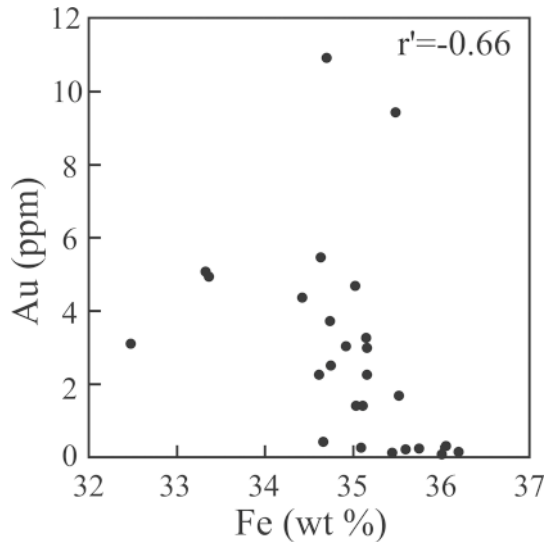


FIG. 12. Binary plot of Au (SIMS) and Fe (EPMA) for arsenopyrite from the Bathurst Mining Camp. An inverse Spearman Rank correlation between Au and Fe ($r' = -0.66$) suggests that the Au substitutes for Fe in the arsenopyrite structure.

rite. Gold also is concentrated around the edges of recrystallized clusters and rhombohedral grains of arsenopyrite. Furthermore, low average As contents of arsenopyrite (30.4 atom % As) have resulted from the liberation of arsenic during metamorphic equilibration.

These results suggest that there was a release of Au from pyrite and arsenopyrite during dynamic metamorphism, which affected the distribution of Au within pyrite and arsenopyrite. Massive sulfide deposits in the BMC have undergone lower- to upper-greenschist metamorphism, with the grade increasing from northeast to southwest (van Staal *et al.* 1992). Rocks in the California Lake Group, which are located in the northwest portion of the Bathurst Mining Camp, are less strongly metamorphosed than those of the Tetagouche Group (Currie *et al.* 2003). However, the Au content of pyrite and arsenopyrite does not appear to be a function of metamorphic grade. Under greenschist conditions of metamorphism (4 to 6 kbar, 400°C; van Staal 1985, Lentz & Goodfellow 1993b, c), Au can be remobilized from massive sulfides. Synmetamorphic deformation likely allowed the release of Au and Ag held in pyrite, and the subsequent precipitation of Au–Ag alloy as inclusions surrounding As-rich regions in pyrite and at the margins of clusters and rhombohedral grains of arsenopyrite.

CONCLUSIONS

Gold in massive sulfide deposits of the Bathurst Mining Camp occurs primarily as a submicroscopic fraction in pyrite and, to a lesser degree, arsenopyrite. Furthermore, granular and colloform pyrite were found to possess higher Au contents than euhedral grains, which have been recrystallized to a much higher degree.

Although Au in the BMC is attributed, for the most part, to solid solution and submicroscopic Au in pyrite and arsenopyrite, other forms of gold not identified in this study may contribute to the overall gold budget. On the basis of the modal abundance of sulfide minerals coupled with their average Au contents, pyrite and arsenopyrite cannot alone account for the bulk Au contents determined in the samples; visible Au may account for the remaining bulk gold in these samples.

Greenschist-facies metamorphism has resulted in the variable recrystallization of massive sulfides. Primary Au in pyrite was consequently released and adsorbed as submicroscopic inclusions of Au–Ag alloy on As-rich surfaces of pyrite and arsenopyrite.

ACKNOWLEDGEMENTS

Secondary-ion mass spectrometry (SIMS) analyses were performed at the Canada Centre for Mineral and Energy Technology in Ottawa with the assistance of Greg McMahon and J.H. Gilles Laflamme. Electron-microprobe analyses were performed at the University of New Brunswick with the help of Douglas Hall. In-

strumental neutron-activation analyses (INAA) were performed by Activation Laboratories Ltd., Ancaster, Ontario. Both INAA and SIMS analyses were funded by an NSERC grant to David Lentz and the New Brunswick Department of Natural Resources and Energy. Major- and trace-element analyses performed at the Geological Survey of Canada, Ottawa, were funded through the EXTECH II project. Scanning electron photomicrographs were funded by Wayne Goodfellow at the Geological Survey of Canada and acquired by Patricia Hunt. Access to drill core was provided by Breakwater Resources Ltd., Heath Steele Mines Ltd., Brunswick Mining and Smelting Ltd. and Noranda Exploration Ltd. This manuscript benefitted from thorough reviews by Tassos Grammatikopoulos, Ilya Vikentyev and the editorial comments of Robert F. Martin.

REFERENCES

- ABBEY, S. (1979): Reference materials – rock samples. *CANMET Report* **79-35**.
- ADAIR, R.N. (1992): Stratigraphy, structure, and geochemistry of the Halfmile Lake massive-sulphide deposit, New Brunswick. *Explor. Mining Geol.* **1**, 151-166.
- BOWMAN, W.S. (1991): Certified reference materials. *CANMET Report* **91-1E**.
- BOYLE, D.R. (1995): Geochemistry and genesis of the Murray Brook precious metal gossan deposit, Bathurst Mining Camp, New Brunswick. *Explor. Mining Geol.* **4**, 341-363.
- BOYLE, R.W. (1979): The geochemistry of gold and its deposits. *Geol. Surv. Can., Bull.* **280**.
- BÜRG, G.H. (1930): Die Sichtbarmachung des feinverteilten Goldes in goldhaltigen Erzen und ihre wirtschaftliche Bedeutung. *Metall und Erz* **27**, 333-338.
- BURTON, D.M. (1993): The Murray Brook (Cu-rich) massive-sulfide deposit, Bathurst Camp, New Brunswick. In *Guidebook to the Metallogeny of the Bathurst Camp* (S.R. McCutcheon & D.R. Lentz, eds.). *Geol. Soc. Can. Inst. Mining Metall., Field Trip* **4**, 135-143.
- CABRI, L.J., CHRYSSOULIS, S.L., DE VILLIERS, J.P.R., LAFLAMME, J.H.G. & BUSECK, P.R. (1989): The nature of “invisible” gold in arsenopyrite. *Can. Mineral.* **27**, 353-362.
- CAVELERO, R.A. (1993): The Caribou massive sulphide deposit, Bathurst Camp, New Brunswick. In *Guidebook to the Metallogeny of the Bathurst Camp* (S.R. McCutcheon & D.R. Lentz, eds.). *Geol. Soc. Can. Inst. Mining Metall., Field Trip* **4**, 115-131.
- CHRYSSOULIS, S.L. & AGHA, U. (1990): Gold mineralogical balance in two Brunswick ore samples. *Surface Science Western, Unpublished report, Univ. of Western Ontario, London, Ontario*.

- _____, CABRI, L.J. & LENNARD, W. (1989): Calibration of the ion microprobe for quantitative trace precious metal analyses of ore minerals. *Econ. Geol.* **84**, 1684-1689.
- COOK, N.J. & CHRYSOULIS, S.L. (1990): Concentrations of "invisible gold" in the common sulfides. *Can. Mineral.* **28**, 1-16.
- CRAIG, J.R. (1983): Metamorphic features in Appalachian massive sulphides. *Mineral. Mag.* **47**, 515-525.
- CURRIE, K.L., VAN STAAL, C.R., PETER, J.M. & ROGERS, N. (2003): Conditions of metamorphism of the main massive sulfide deposits and surrounding rocks in the Bathurst Mining Camp. In *Massive Sulfide Deposits in the Bathurst Mining Camp, New Brunswick and Northern Maine* (W.D. Goodfellow, S.R. McCutcheon & J.M. Peter, eds.). *Econ. Geol., Monogr.* **11**, 65-78.
- DE ROO, J.A. & VAN STAAL, C.R. (2003): Sulfide remobilization and sulfide breccias in the Heath Steele and Brunswick deposits, Bathurst Mining Camp, New Brunswick. In *Massive Sulfide Deposits in the Bathurst Mining Camp, New Brunswick and Northern Maine* (W.D. Goodfellow, S.R. McCutcheon & J.M. Peter, eds.). *Econ. Geol., Monogr.* **11**, 479-496.
- FLEET, M.E., MACLEAN, P.J. & BARBIER, J. (1989): Oscillatory-zoned As-bearing pyrite from strata-bound and stratiform gold deposits: an indicator of ore fluid evolution. In *The Geology of Gold Deposits: The Perspective in 1988* (R.R. Keays, W.R.H. Ramsay & D.I. Groves, eds.). *Econ. Geol., Monogr.* **6**, 356-362.
- GAMMONS, C.H. & WILLIAMS-JONES, A.E. (1995): The solubility of Au-Ag alloy + AgCl in HCl/NaCl solutions at 300°C: new data on the stability of Au(I) chloride complexes in hydrothermal fluids. *Geochim. Cosmochim. Acta* **59**, 3453-3468.
- GENKIN, A.D., BORTNIKOV, N.S., CABRI, L.J., WAGNER, F.E., STANLEY, C.J., SAFONOV, Y.G., MCMAHON, G., FRIEDL, J., KERZIN, A.L. & GAMYANIN, G.N. (1998): A multidisciplinary study of invisible gold in arsenopyrite from four mesothermal gold deposits in Siberia, Russian Federation. *Econ. Geol.* **93**, 463-487.
- GOODFELLOW, W.D. (1975): Major and minor element halos in volcanic rocks at Brunswick No. 12 sulphide deposit, N.B., Canada. In *Geochemical Exploration 1974* (I.L. Elliot & W.K. Fletcher, eds.). Elsevier, Amsterdam, The Netherlands (279-295).
- _____. (2003): Geology and genesis of the Caribou deposit, Bathurst Mining Camp, New Brunswick, Canada. In *Massive Sulfide Deposits in the Bathurst Mining Camp, New Brunswick and Northern Maine* (W.D. Goodfellow, S.R. McCutcheon & J.M. Peter, eds.). *Econ. Geol., Monogr.* **11**, 327-360.
- _____ & MCCUTCHEON, S.R. (2003): Geologic and genetic attributes of volcanic sediment-hosted massive sulfide deposits of the Bathurst Mining Camp, northern New Brunswick – a synthesis. In *Massive Sulfide Deposits in the Bathurst Mining Camp, New Brunswick and Northern Maine* (W.D. Goodfellow, S.R. McCutcheon & J.M. Peter, eds.). *Econ. Geol., Monogr.* **11**, 245-302.
- HANNINGTON, M.D. & GORTON, M.P. (1991): Analysis of sulfides for gold and associated trace metals by direct neutron activation with a low-flux reactor. *Geostandards Newsletter* **15**, 145-154.
- _____, PETER, J.M. & SCOTT, S.D. (1986): Gold in sea-floor polymetallic sulfide deposits. *Econ. Geol.* **81**, 1867-1883.
- _____ & SCOTT, S.D. (1989): Gold mineralization in volcanogenic massive sulfides: implications of data from active hydrothermal vents on the modern seafloor. In *The Geology of Gold Deposits: the Perspective in 1988* (R.R. Keays, W.R.H. Ramsay & D.I. Groves, eds.). *Econ. Geol., Monogr.* **6**, 491-507.
- HEALY, R.E. & PETRUK, W. (1990): Petrology of Au-Ag-Hg alloy and "invisible" gold in the Trout Lake massive sulfide deposit, Flin Flon, Manitoba. *Can. Mineral.* **28**, 189-206.
- HELMSTAEDT, H. (1973): Structural geology of the Bathurst-Newcastle district. *New England Intercollegiate Geological Conference, Field Guide* **5-A**, 34-46.
- HUSTON, D.L., BOTTRILL, R.S., CREELMAN, R.A., ZAW, K., RAMSDEN, T.R., RAND, S.W., GEMMELL, J.B., JABLONSKI, W., SIE, S.H. & LARGE, R.R. (1992): Geological and geochemical controls on the mineralogy and grain size of gold bearing phases, eastern Australian volcanogenic massive sulfide deposits. *Econ. Geol.* **87**, 542-563.
- _____ & LARGE, R.R. (1989): A chemical model for the concentration of gold in volcanogenic massive sulphide deposits. *Ore Geol. Rev.* **4**, 171-200.
- KRETSCHMAR, U. & SCOTT, S.D. (1976): Phase relations involving arsenopyrite in the system Fe-As-S and their application. *Can. Mineral.* **14**, 364-386.
- LARGE, R.R. (1977): Chemical evolution and zonation of massive sulfide deposits in volcanic terrains. *Econ. Geol.* **72**, 549-572.
- LAROCQUE, A.C.L., HODGSON, C.J., CABRI, L.J. & JACKMAN, J.A. (1995): Ion-microprobe analysis of pyrite, chalcopyrite and pyrrhotite from the Mobern VMS deposit in northwestern Quebec: evidence for metamorphic remobilization of gold. *Can. Mineral.* **33**, 373-388.
- LEBLANC, S. (1989): *Massive Sulphide-Associated Gold: Brunswick No. 12 Mine, Bathurst, New Brunswick*. B.Sc. Honours thesis, Univ. of New Brunswick, Fredericton, New Brunswick.
- LENTZ, D.R. (1995): Preliminary evaluation of six in-house rock geochemical standards from the Bathurst Camp, New Brunswick. In *Current Research 1995* (S.A.A. Merlini, ed.). *New Brunswick Department of Natural Resources and Energy, Minerals and Energy Division, Misc. Rep.* **18**, 81-89.

- _____ (1999): Deformation-induced mass transfer in felsic volcanic rocks hosting the Brunswick No. 6 massive-sulfide deposit, New Brunswick: geochemical effects and petrogenetic implications. *Can. Mineral.* **37**, 489-512.
- _____ (2002): Sphalerite and arsenopyrite at the Brunswick No. 12 massive sulfide deposit, Bathurst Camp, New Brunswick: constraints on P-T evolution. *Can. Mineral.* **40**, 19-31.
- _____ & GOODFELLOW, W.D. (1993a): Geochemistry of the stringer sulphide zone in the discovery hole at the Brunswick No. 12 massive sulphide deposit, Bathurst, New Brunswick. *Geol. Surv. Can., Pap.* **93-1E**, 259-269.
- _____ & _____ (1993b): Mineralogy and petrology of the stringer sulphide zone in the discovery hole at the Brunswick No. 12 massive sulphide deposit, Bathurst, New Brunswick. *Geol. Surv. Can., Pap.* **93-1E**, 249-258.
- _____ & _____ (1993c): Petrology and mass-balance constraints on the origin of quartz-augen schist associated with the Brunswick massive sulfide deposits, Bathurst, New Brunswick. *Can. Mineral.* **31**, 877-903.
- LUFF, W.M. (1995): A history of mining in the Bathurst area, northern New Brunswick, Canada. *Can. Inst. Mining Metall., Bull.* **88**(994), 63-68.
- _____, GOODFELLOW, W.D. & JURAS, S.J. (1992): Evidence for a feeder pipe and associated alteration at the Brunswick No. 12 massive sulphide deposit. *Explor. Mining Geol.* **1**, 167-185.
- MARSHALL, B. & GILLIGAN, L.B. (1987): An introduction to remobilization: information from ore-body geometry and experimental considerations. *Ore Geol. Rev.* **2**, 87-131.
- MCALLISTER, A.L. (1960): Massive sulphide deposits in New Brunswick. *Can. Inst. Mining Metall., Bull.* **53**(574), 88-98.
- McCLENAGHAN, S.H. (2002): *Gold in Massive Sulphide Deposits, Bathurst Mining Camp, New Brunswick: Form, Distribution and Genesis*. M.Sc. thesis, Univ. of Ottawa, Ottawa, Ontario.
- _____, GOODFELLOW, W.D. & LENTZ, D.R. (2003): Gold in massive sulfide deposits, Bathurst Mining Camp: distribution and genesis. In *Massive Sulfide Deposits in the Bathurst Mining Camp, New Brunswick and Northern Maine* (W.D. Goodfellow, S.R. McCutcheon & J.M. Peter, eds.). *Econ. Geol., Monogr.* **11**, 303-326.
- McCUTCHEON, S.R., WALKER, J.A. & McCLENAGHAN, S.H. (2001): The geological settings of massive sulphide deposits in the Bathurst Mining Camp: a synthesis. In *Current Research 2000* (B.M.W. Carroll, ed.). *New Brunswick Department of Natural Resources and Energy, Minerals and Energy Division, Mineral Resource Rep.* **4**, 63-95.
- McMAHON, G. & CABRI, L.J. (1998): The SIMS technique in ore mineralogy. In *Modern Approaches to Ore and Environmental Mineralogy* (L.J. Cabri & D.J. Vaughan, eds.). *Mineral. Assoc. Can., Short Course* **27**, 199-224.
- PISUTHA-ARNOND, V. & OHMOTO, H. (1983): Thermal history, and chemical and isotopic compositions of the ore-forming fluids responsible for the Kuroko massive sulfide deposits in the Hokuroku District of Japan. In *The Kuroko and Related Volcanogenic Massive Sulfide Deposits* (H. Ohmoto & B.J. Skinner, eds.). *Econ. Geol., Monogr.* **5**, 523-558.
- ROBINSON, B.W., WARE, N.G. & SMITH, D.G.W. (1998): Modern electron-microprobe trace-element analysis in mineralogy. In *Modern Approaches to Ore and Environmental Mineralogy* (L.J. Cabri & D.J. Vaughan, eds.). *Mineral. Assoc. Can., Short Course* **27**, 153-180.
- SHIKAZONO, N. & SHIMIZU, M. (1987): The Ag/Au ratio of native gold and electrum and the geochemical environment of gold vein deposits in Japan. *Mineral. Deposita* **22**, 309-314.
- STANTON, R.L. (1960): General features of the conformable "pyritic" orebodies. I. Field association. *Can. Inst. Mining Metall., Bull.* **53**(573), 24-29.
- SUTHERLAND, J.K. (1967): The chemistry of some New Brunswick pyrites. *Can. Mineral.* **9**, 71-84.
- VAN STAAL, C.R. (1985): *The Structure and Metamorphism of the Brunswick Mines Area, Bathurst, New Brunswick, Canada*. Ph.D. thesis, Univ. of New Brunswick, Fredericton, New Brunswick.
- _____ & FYFFE, L.R. (1991): Dunnage and Gander zones, New Brunswick: Canadian Appalachian Region. *New Brunswick Dep. of Natural Resources and Energy, Minerals Resources, Geosci. Rep.* **91-2**.
- _____, _____, LANGTON, J.P. & McCUTCHEON, S.R. (1992): The Ordovician Tetagouche Group, Bathurst Camp, northern New Brunswick, Canada: history, tectonic setting, and distribution of massive-sulfide deposits. *Explor. Mining Geol.* **1**, 93-103.
- _____, RAVENHURST, C.E., WINCHESTER, J.A., RODDICK, J.C. & LANGTON, J.P. (1990): Post-Taconic blueschist suture in the northern Appalachians of northern New Brunswick, Canada. *Geology* **18**, 1073-1077.
- WAGNER, F.E., MARION, P. & REGNARD, J.R. (1986): Mössbauer study of the chemical state of gold in gold ores. In *Gold 100, Proc. Int. Conf. Gold. 2. Extractive Metallurgy of Gold*. *S. Afr. Inst. Mining Metall.*, 435-443.

Received November 7, 2003, revised manuscript accepted March 3, 2004.

APPENDIX. RESULTS OF SIMS ANALYSES FOR Au (ppm) IN PYRITE AND ARSENOPYRITE FROM SELECTED DEPOSITS, BATHURST MINING CAMP, NEW BRUNSWICK

Pyrite (day 1)		Pyrite (day 2)		Arsenopyrite (day 3)	
1 Orvan Brook	2.36	38 Louvicourt	2.40	1 Rocky Turn	0.18
2	5.01	39	3.34	2	0.26
3	2.56	40	9.81	3	0.25
5	2.21	41	11.67	4	0.24
6	5.60	42	3.63	5	0.13
7	5.49	43	6.18	6	0.11
8	4.27	44	42.87	7	0.12
9	<0.53	45	10.36	8 Orvan Brook	3.73
10	<0.53	46	11.02	9	2.24
11 Restigouche	2.51	47	0.74	10	5.02
12	1.79	48	8.37	11	9.42
13	2.81	49 Murray Brook	6.92	12	4.67
14	3.47	50	9.96	13	3.25
15	5.78	51	11.92	14	2.49
16	1.90	52	24.28	15	3.05
17	8.41	53	19.90	16	2.98
18	1.88	54	29.55	17	4.35
19	10.32	55	27.26	18	2.57
20	1.52	56	32.04	19 Heath Steele	1.71
21	10.67	57	11.07	20 B zone	0.42
22	4.47	59	20.67	21 Bedded Sulfide	3.14
23	7.55	60	11.48	22 Murray Brook	5.44
24	23.74	61	0.56	23	10.91
25	10.88	62 Stratmat Main	3.80	24	4.95
26	6.72	63	4.75	25	2.22
27 Rocky Turn	16.22	64	2.40	26	1.43
28	19.25	65	0.48	27	1.40
29	25.91	66	5.17		
30	31.95	67	2.33		
31 Heath Steele	9.26	68	2.99		
32 B zone	1.20	69	3.71		
33 Bedded Sulfide	12.73	70 Canoe Landing	2.08		
34	10.62	71 Lake	2.70		
35	19.90	72	11.71		
36	9.88	73	19.53		
37	<0.53	74 Heath Steele	1.32		
		75 B zone Sulfide	1.24		
		76 Fragmental	0.66		
		77	3.46		

Day 1: Minimum detection-level for analyses 1-37 is 532 ppb (number 4 discarded owing to improper mineral.

Day 2: Minimum detection-level for analyses 38-77 is 452 ppb (number 58 discarded owing to improper mineral.

Day 3: Minimum detection-level for analyses 1-27 is 92 ppb.